Doctoral Thesis

The function of ITGBL1 in the process of cartilage formation and its potential as a therapeutic agent for cartilage disease.

Eun kyung Song

School of Life Sciences
(Biological Sciences)
Graduate School of UNIST

The function of ITGBL1 in the process of cartilage formation and its potential as a therapeutic agent for cartilage disease.

A thesis submitted to the Graduate School of UNIST in partial fulfillment of the requirements for the degree of Doctor of Science

Eun kyung Song

13.12.2018

Approved by

Advisor

Tae Joo Park

A thesis submitted to the Graduate School of UNIST in partial fulfillment of the requirements for the degree of Doctor of Science

Eun kyung Song

This certifies that the thesis of E.K.Song is approved.

13.12.2018

Advisor: Tae Joo Park

Tae Joo Park

Taejook Kwon

Hyun-Shik Lee

Chan Young Park

Jeong Beom Kim

Contents

Contents ----------1

Abstract ---------- 3

List of figures ---------- 5

Abbreviations ---------- 6

Chapter 1. Introduction

1-1. Patterning the *Xenopus* embryo development

1-1-1. An overview of using *Xenopus laevis* as a model system ---------- 8

1-1-2. An overview of *Xenopus* embryo development ---------- 10

1-1-3. Craniofacial development ---------- 12

1-2. Chondrogenesis

1-2-1. Definition of chondrogenesis ---------- 14

1-2-2. Integrin ---------- 16

1-2-3. Integrin signaling ---------- 19

1-3. ITGBL1

1-3-1. ITGBL1 structure ---------- 20

Chapter 2. ITGBL1 modulates integrin activity to promote cartilage formation and protect against arthritis

2-1. Introduction ---------- 21

2-2. Materials and methods ---------- 23

2-3. Results ---------- 28

2-4. Discussion ---------- 60

Chpater3. Concluding and Remarks

3.1 Summary and Conclusions ---------- 64

Supplements ---------- 66

Acknowledgement ---------- 74

References ---------- 76

Abstract

In general, facial bones are not formed as bones from the beginning. Bone formation occurs through endochondral bone formation process after cartilage is formed. Frog face is simpler than human or mouse, so it is easy to find which gene is involved in facial formation. For this reason, experiments were conducted on *Xenopus laevis* and other experimental animals. The cell is not a major component of cartilage, but the extracellular matrix secreted from the chondrocyte is the main component that gives the elasticity and stiffness of cartilage tissue [1]. In order to complete cartilage tissue, cartilage cells continuously interact with the extracellular matrix surrounding the cells, and the process of secreting cartilage matrix must be accompanied for a long time. This process of forming cartilage tissue is called chondrogenesis. Recent studies have shown that chondrocytes interact with extracellular matrix through various types of integrin molecules, the integrin signal is differentially regulated according to the differentiation of chondrocytes and the state of the cartilage, which helps the cartilage cells to recognize the surrounding environment [2]. It is also known that the integrin signal can induce cartilage-related diseases as well as cartilage differentiation. Integrin signaling is one for the major sources of damage to articular cartilage by amplifying the inflammatory response in both rheumatoid arthritis and osteoarthritis. Fragmented cartilage ECMs combine with synovial fibroblasts and integrins of immune cells in cartilage tissues to exacerbate the inflammatory response by increasing catabolic factor secretion such as IL-6, 8, and MMP [3-6]. To investigate the process of cartilage formation, we analyzed the genes that differentiation into facial cartilage by expressing in cartilage cells of *Xenopus laevis*. In this research, we have discovered that a novel secreted protein ITGBL1 promotes cartilage formation by modulating integrin-ECM interactions during chondrogenesis in a model animal and human bone marrow stem cell. Further ITGBL1 inhibited catabolic signals induced by IL-1β treatment in primary

chondrocytes. We believe ITGBL1 possesses dual functions which promote cartilage formation and inhibit catabolic signals in chondrocytes simultaneously. In this study first identified the function of ITGBL1 protein, which regulates integrin signaling in cartilage formation and chondrocyte differentiation and found that ITGBL1 protein also inhibits cartilage damage and promotes cartilage regeneration in arthritic conditions.

List of figures

Chapter 1. Introduction

Figure 1-1. Overview of *Xenopus laevis*

Figure 1-2. Transplantation of nuclei from blastula cells

Figure 1-3. The relationship of the embryonic dorsal axis to the definitive dorsal axis

Figure 1-4. Characteristic of *Xenopus laevis* early development.

Figure 1-5. ITGBL1 domain

Figure 1-6. Process of Chondrogenesis

Figure 1-7. Schematic model of RhoA and YAP/TAZ relation

Figure 1-8. Structure of Integrin

Figure 1-9. Structure of ITGBL1

Figure 1-10. Schematic of integrin signaling

Chapter 2. ITGBL1 modulates integrin activity to promote cartilage formation and protect against arthritis

Figure 2-1. ITGBL1 is involved in facial cartilage development

Figure 2-2. ITGBL1 function in chondrogenic differentiation of human bone marrow stem cells(BMSCs) and mouse limb-bud mesenchymes

Figure 2-3. ITGBL1 inhibits integrin-ECM complex formation in PC3 cells

Figure 2-4. ITGBL1 inhibits integrin-ECM complex formation in various cell types including chondrocytes

Figure 2-5. ITGBL1 promotes chondrogenesis via integrin inhibition

Figure 2-6. ITGBL1 protects chondrocytes from catabolic gene expression

Abbreviations

ITGBL1: Integrin beta-like protein 1

EGF: epidermal growth factor

OA: osteoarthritis

ECM: extracellular matrix

RGD: Arginylglycylaspartic acid

BMSC: bone marrow mesenchymal stem cell

Fn-f: fibronectin fragment

Mmp3: matrix metalloproteinase-3

Adamts5: Thrombospondin motifs 5

FAK: focal adhesion kinase

DMM: destabilization of the medial meniscus

OARSI: osteoarthritis research society international

Bglap2: bone gamma-carboxyglutamate protein 2

Ibsp: integrin binding sialoprotein

TGF-β: transforming growth factor-β

MBT: mid-blastula transition

PCP: planar cell polarity

PKC: protein kinase C

YAP: yes-associated protein

MAPK: mitogen-activated protein kinase

Sox9: sex-determining region Y-Box 9 protein

Col2a1: collagen, type II, alpha 1

Col10a1: collagen, type X, alpha 1

Ihh: Indian hedgehog

PC3: human prostate cancer cell

FACS: fluorescence-activated cell sorting

ERK1/2: extracellular signal-regulated kinase 1/2

Cox-2: cycloozygenase-2

Bio1211: integrin-α4β1 inhibitor

Obtustatin: integrin-α1β1 inhibitor

ATN-161: integrin-α5β1 inhibitor

IL-1β: interleukin 1 β

MMR: Marc's Modified Ringer's

MTT: 3-(4,5-dimethylthiazol-2-yl)-2,5diphenyltetrazolium bromide

Chapter 1. Introduction

1-1. Patterning the *Xenopus* embryo development

1-1-4. An overview of using *Xenopus laevis* as a model system

Figure 1-1. Overview of *Xenopus laevis*

Xenopus laevis is one of the animals with the longest history as an experimental animal with Drosophila. One of the model systems with important contributions is *Xenopus laevis*, the African clawed frog, a pseudotetraploid vertebrate which lives in fresh water. The reason why it is used globally in research is the high level of conservation of the most basic cellular and molecular mechanisms, it can be easily manipulated at low cost and it is easy to obtain large quantities of substances through various experimental procedures. A life cycle that among Amphibian is relatively short, large number and size of eggs suitable for microsurgery, and above all its year-round reproductive response to commercial hormone

preparations compared to the limited breeding seasons of other amphibians [7], [8]. The *Xenopus laevis* ovary is large, transparent and can easily contain hundreds of large oocytes. Like other model systems used in embryology, *Xenopus* oocytes can be used to facilitate transplantation [9], [10]. Because of the large size of the oocyte, enucleation can be easily handled. Morpholino or siRNA can be injected into the oocyte to inhibit the expression of the gene of interest and to examine its function.

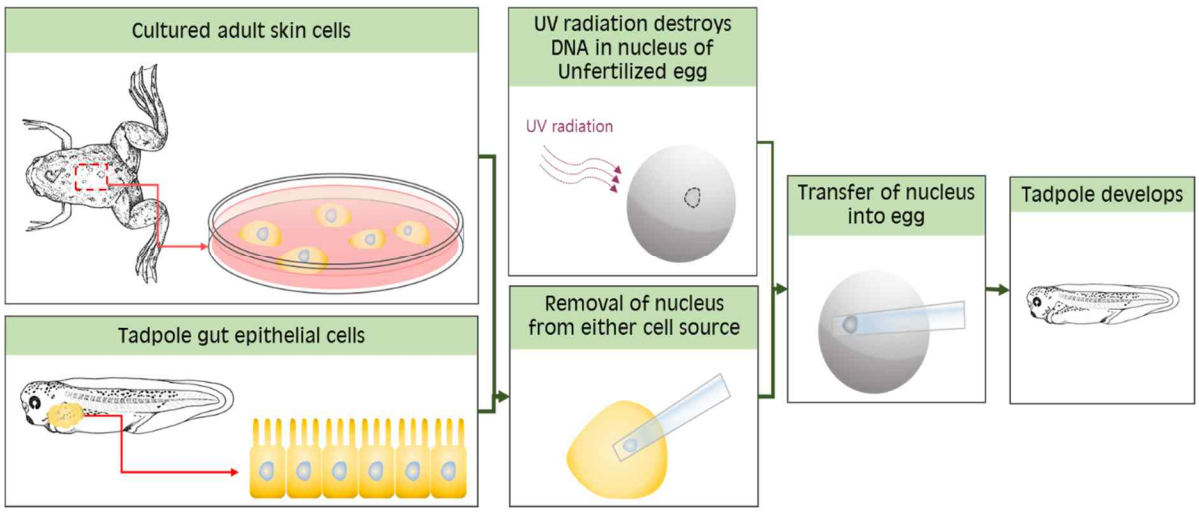

Figure 1-2. Transplantation of nuclei from blastula cells

In addition, *Xenopus* model system can be used in various fields such as chromatin studies small molecule inhibitor screening, microscopy, and drug screening.

1-1-2. An overview of *Xenopus* embryo development

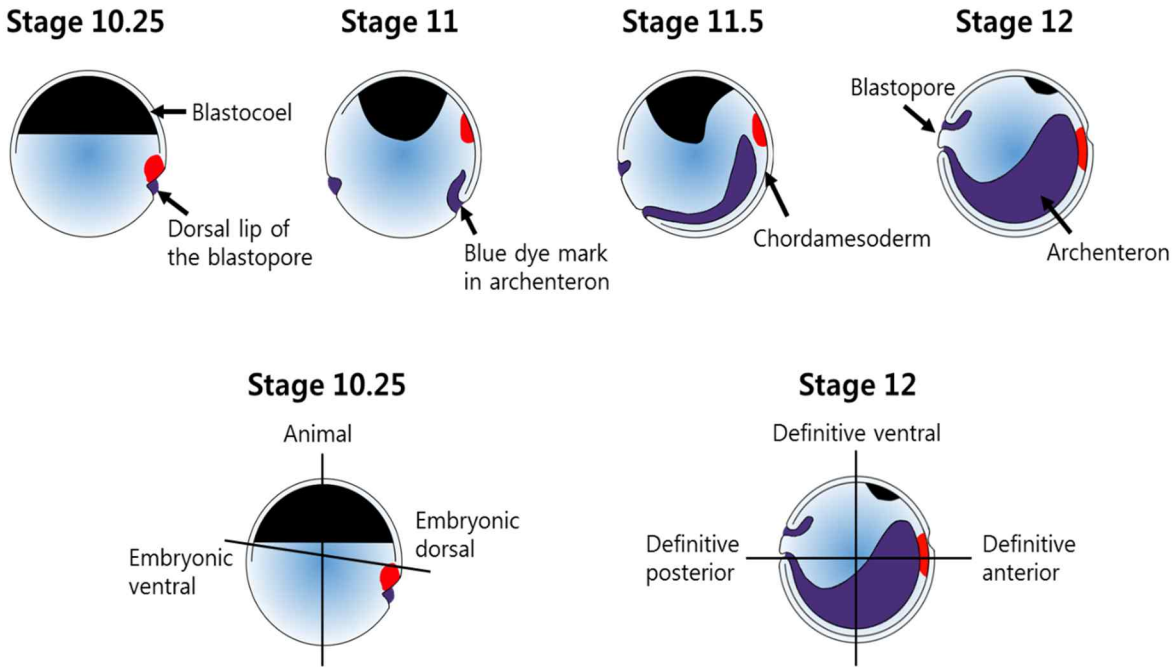

Figure 1-3. The relationship of the embryonic dorsal axis to the definitive dorsal axis

Generation of *Xenopus* starts from axis formation. The first axis of the *Xenopus* embryo is the animal-vegetal axis, which passes through the animally localized egg pro-nucleus, the center of the egg and the vegetal poles (Fig. 1-3). The second axis is defined as the sperm penetration point and migration of the cortical cytoplasm to the furthest point from the sperm entry point.

After fertilization, the *Xenopus* embryo must undergo a cell cycle to have distinctive functions. (Fig. 1-3). During the first, 1hour 30minute cell cycle, cortical movement and pro-nuclear fusion of male and female occur. And 4000 cells were formed by eleven cleavages for 20-30 minutes, which fill the blastocoel cavity. The embryo, which is 50-90 minutes later, is called

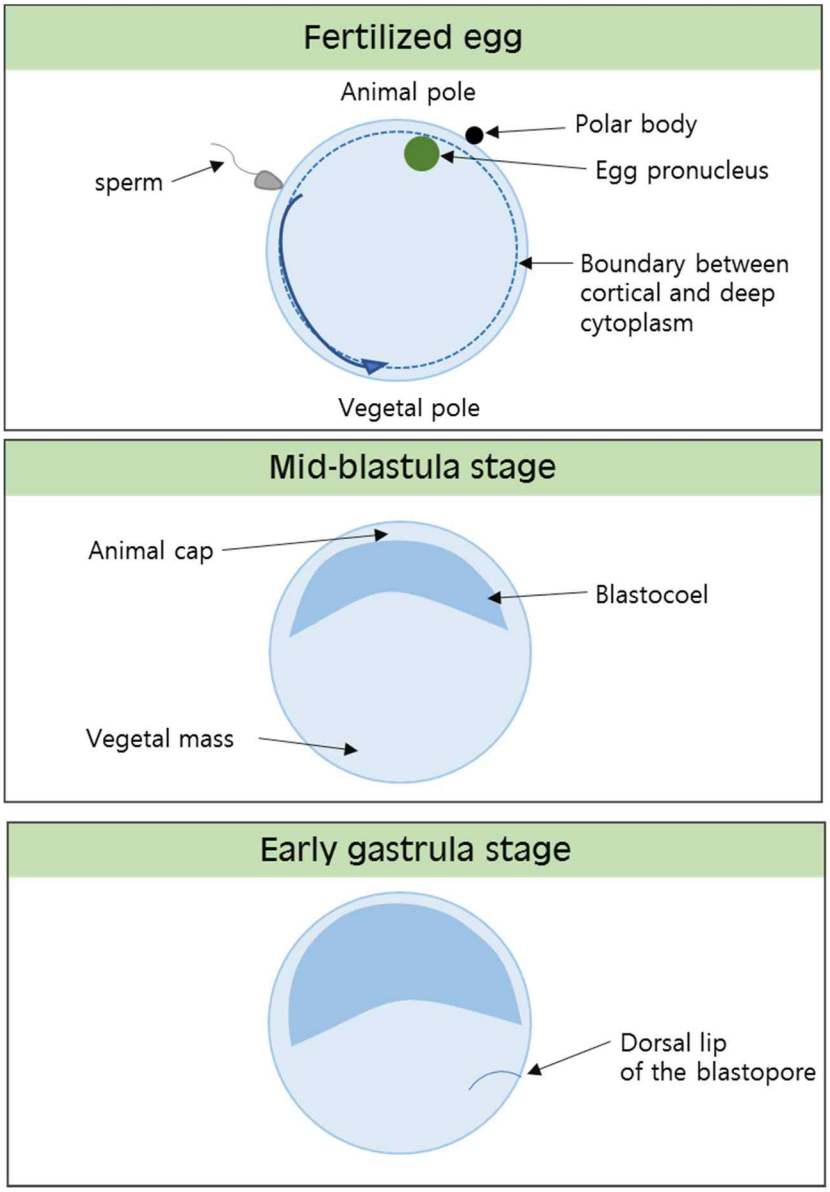

Figure 1-4. Characteristic of *Xenopus laevis* early development

the mid-blastula stage has 3 layers, the animal cap, the marginal zone, and the vegetal mass.

Next, the process called MBT(mid-blastula transition) starts the zygotic gene transcription. And then dorsal lip of blastopore is formed, gastrulation starts, and mitosis stops. By this gastrulation, the rounded embryo is transformed into three layers and forms what is called anteroposterior and dorsoventral(DV) axis [11].

1-1-3. Craniofacial development

The vertebrate head has a very complicated structure. In order to form a craniofacial, a tissue-tissue interaction between the derivation of all germ layers and the harmonic morphogenetic movements of three dimensions is required. Generally, the development of a craniofacial structure involves separate steps followed by germ layer patterning. First, the neural crest is induced at the ectoderm, neuroectoderm border. This is followed by movement of the cranial neural crest into the presumptive facial primordia [12], [13], [14], [15], [16]. During development of vertebrate craniofacial, neural crest cells contribute to cartilage, bone and connective tissue development to form the face. This neural crest cell is a vertebrate specific cell population derived from the dorsal part of the neural tube. Following induction, neural crest cells delaminate and migrate to different regions of the embryo, where they differentiate into a broad range of cell types, including peripheral and enteric neurons, glia, melanocytes and smooth muscle [17], [18], [19]. Furthermore, in the cranial region, neural crest cell contributes to the cartilage and bone formation of the skull, face and pharyngeal skeletons. Interactions between neural crest cells and their local environment are crucial in cranial neural crest cells directional migration [20]. The non-canonical Wnt, planar cell polarity signaling pathway and cell-cell interaction are involved in controlling the polarity of migrating neural crest cells. As the neural crest migrates into the face, the cranial placodes, which are specialized ectodermal thickening, differentiate. The moving neural crest cells determines the final destination through the surrounding signal. For example, in the case of *Xenopus*, *Twist*

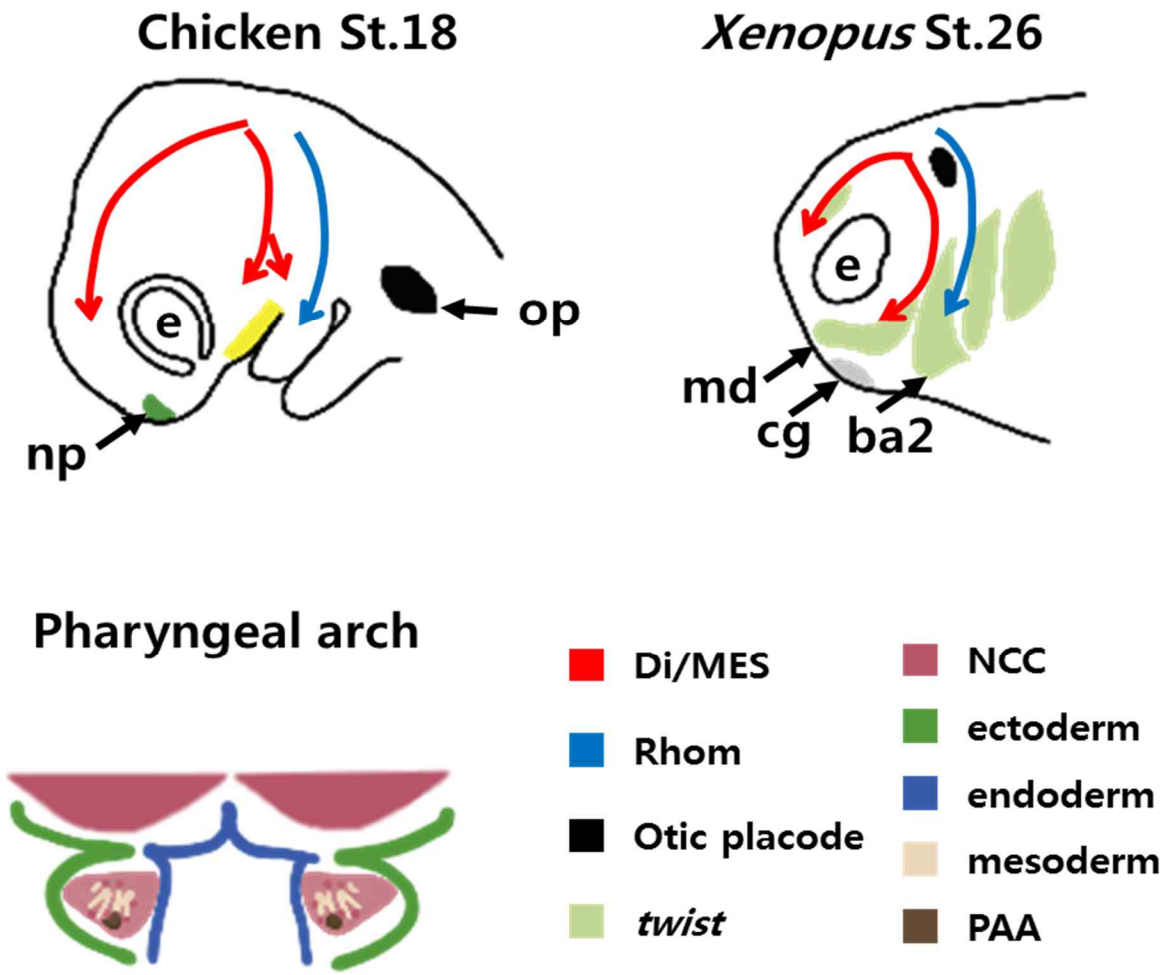

Figure 1-5. Craniofacial anatomy

marks the end position of the cranial neural crest. These signals are preserved between species.

Subsequently, regional spread of neural crest forms facial prominences. In the pharyngeal arches (also called branchial arches) phase of the early stages, vertebrate embryos have substantial morphological homology [21], [22]. The pharyngeal arch is a metameric structure composed of the ectoderm and endoderm. Mandibular primordium or lower jaw occurs form the first pharyngeal arch [23], [22], [21], [24], [25].

Next, the facial prominences fuse to presage the mature form of the face. Finally, the skeleton of the face is formed.

1-2. Chondrogenesis

1-2-1. Definition of chondrogenesis

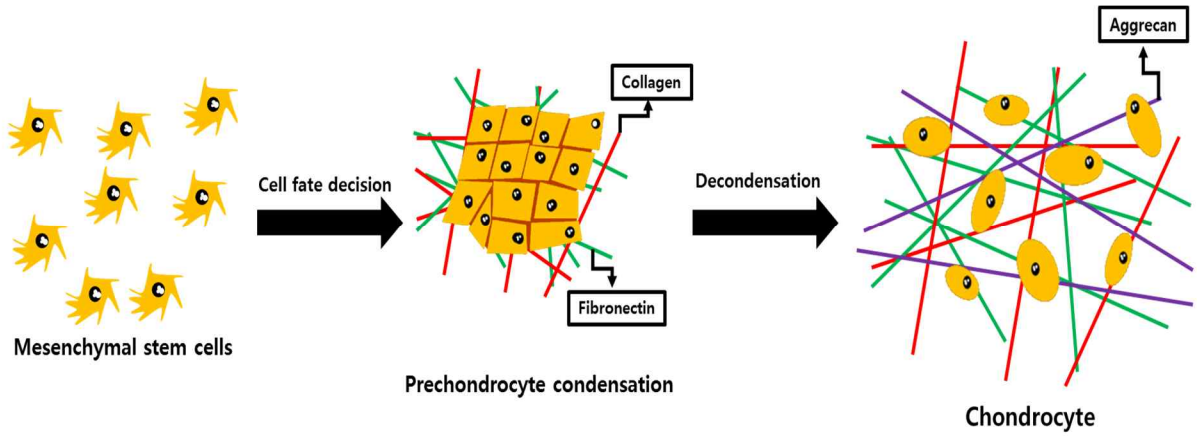

Figure 1-6. Process of Chondrogenesis

Chondrogenesis (also known as chondrification) is the process of cartilage formation. Chondrogenesis occurs as a result of mesenchymal cell condensation and chondroprogenitor cell differentiation. By chondrogenesis, chondrocyte proceeds the formation of articular cartilage or undergo proliferation, terminal differentiation to chondrocyte hypertrophy, and apoptosis in a process termed endochondral ossification [26]. The chondrogenesis begins with the condensation of prechondrocyte [27, 28]. This initial condensation mediated by both cell-cell adhesion and cell-ECM interaction [29]. Then, condensed prechondrocytes are dissociated while secreting cartilage-specific ECM molecules. During this de-condensation process, prechondrocytes have become round shaped mature chondrocytes. Actin cytoskeleton plays an important role in this chondrogenesis. There are two downstream mechanisms that regulate cytoskeletal regulation in chondrogenesis. First, PKC and ERK1 function as downstream

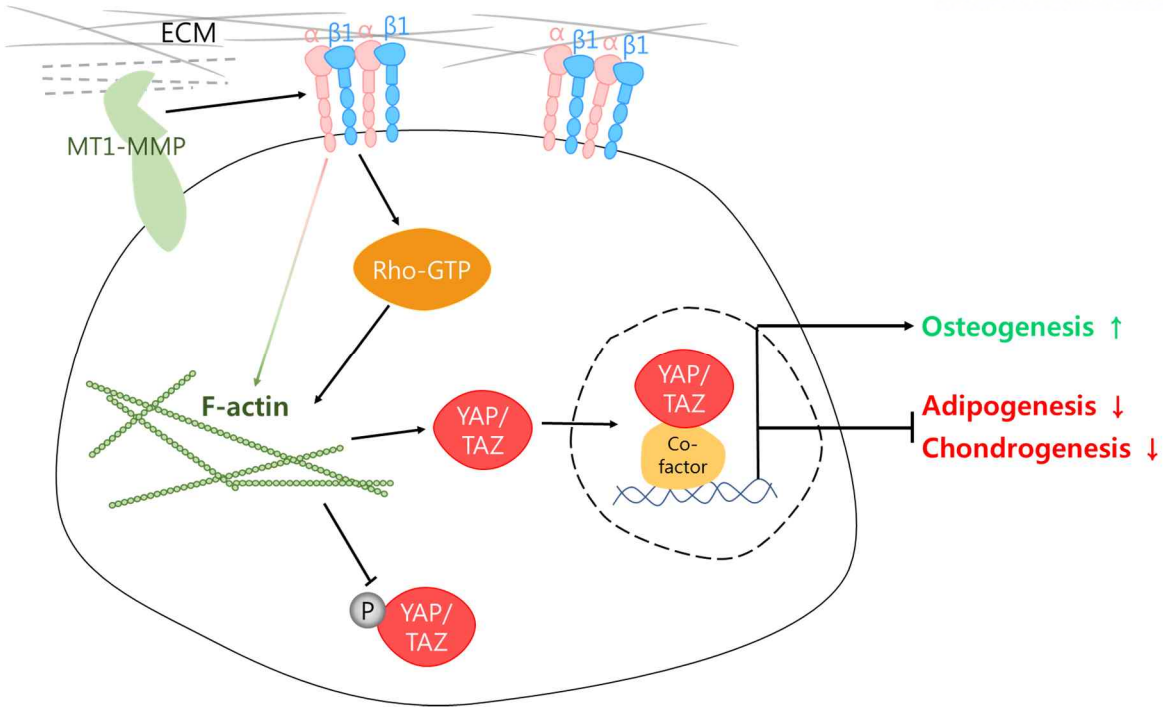

Figure 1-7. Schematic model of RhoA and YAP/TAZ relation

effectors [30]. And the YAP/TAZ transcription factor RhoA signaling [31]. The factors mentioned above are involved in chondrogenesis through regulation of actin cytoskeleton and mechanical signaling. MAPKs(including ERK, c-Jun N-terminal kinase, and p38) are also an important regulator of chondrogenesis. Among them, it is regulated by integrin which is an upstream of MAPK and ERK1/2 and p38 factors which are downstream of MAPK.

1-2-2. Integrin

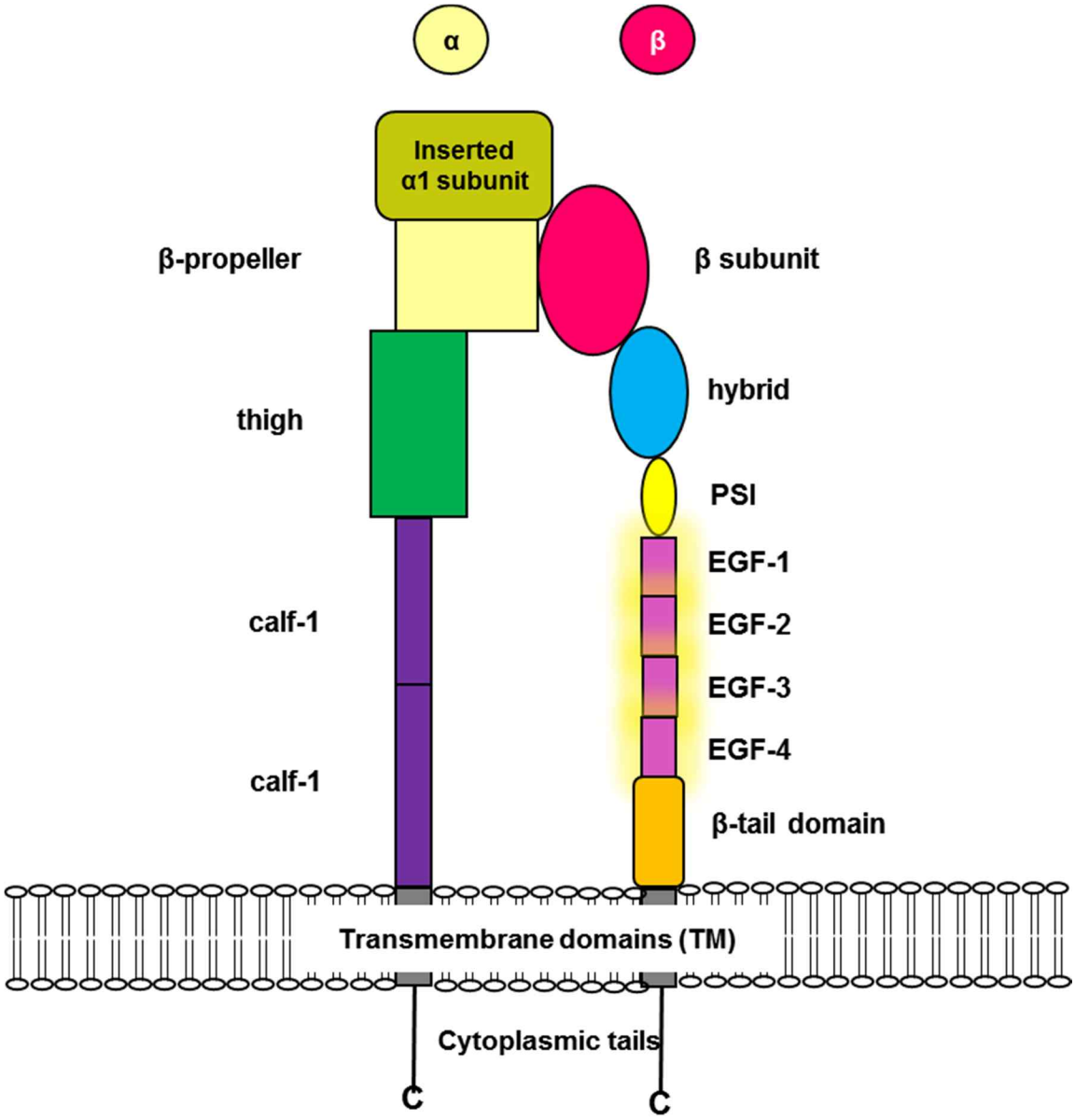

Figure 1-8. Structure of integrin

Integrins are several kinds of α chain and β chain, and there are more than 24 integrins depending on the combination of α chain and β chain. Each αβ combination has its own binding specificity and signaling properties. Most integrins recognize a variety of ECM proteins, such as fibronectin, laminins, collagens, and vitronectins [32].

Integrin is a dimer composed of two strands of α chain and β chain, and is a type I membrane protein having a short C-terminal structure and an extracellular long N-terminal structure. The extracellular domain is present in a state where cations such as Ca^{2+} and Mg^{2+} are bound [33]. Ligands for integrins include fibronectin, vitronectin, collagen, laminin, and the like [32]. Outside-in activation, when the RGD peptide of an artificial ligand bind to the extracellular domain of the integrin, the closed dimer is opened in an unfolded state (extended state). As a result, the intracellular domain of the integrin is also open. Then the talin can bind to the C-terminus of the open integrin [34], [35]. This bond induces assembly of actin filaments connected to the C-terminal of the integrin. Conversely, in the inside-out activation, when talin is attached to the C-terminus of the integrin, the structure of the integrin is changed and the extracellular region is opened and the affinity for the ligand is increased. The function of integrins can be broadly divided into the transfer of extracellular changes detected through extracellular matrix into cells and the attachment of cells to extracellular matrix. Specific functions include cell migration, surveillance of immune cells, and blood clotting, in which fibrinogen in the blood binds to GPIIbIIIa [36]. Immobilization to extracellular matrix is the most basic and essential process in multicellular organisms. This ensures the stabilization of the cells and allows not only immobilization to the ECM, but also signal transmission between the extracellular and intracellular regions. In addition to talin, vinculin, paxillin, and α-actinin are required for this signal transduction [37].

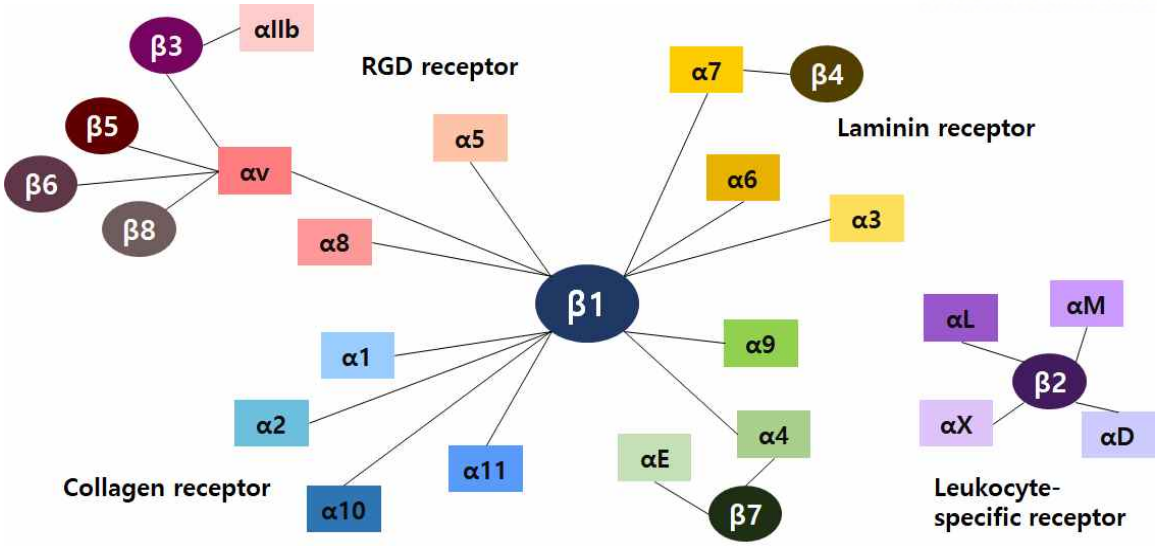

Figure 1-9. Subtype of Integrin

1-2-3. Integrin signaling

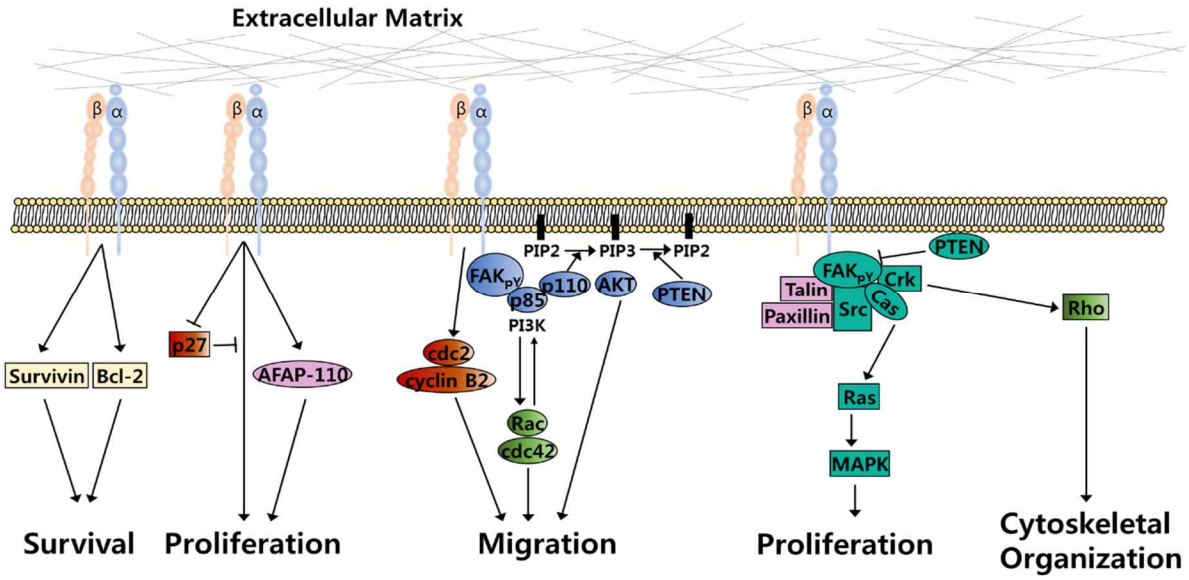

Figure 1-10. Schematic of integrin signaling

Integrin signaling refers to the signal transduction pathways in which integrins at the cell surface respond to mechanical or biochemical stimuli in the extracellular matrix and transmit this information intracellularly to elicit appropriate responses. Integrin signaling is involved in processes including embryonic development, tissue remodeling, and repair, host defense, hemostasis, cell migration, proliferation and regulation of cellular shape. Integrin acts as a bridge between cells and ECM to the intracellular actin cytoskeleton, providing the mechanical basis for anchorage, cell shape determination, force transmission, and migration. Cell-mediated chemical or mechanical changes are transferred into the cell, causing the intracellular signaling reaction to occur, thereby changing the cell cycle, cell shape, and movement (outside-in activation). On the contrary, it also transmits the changes inside the cells out-of-cell (inside-out activation) [38]. The diverse signaling mechanisms triggered by ligand-binding includes enzyme phosphorylation, calcium influx and activation of Rho GTPases, which all together influence all aspects of cell physiology [39].

1-3. ITGBL1(Integrin beta like protein 1)

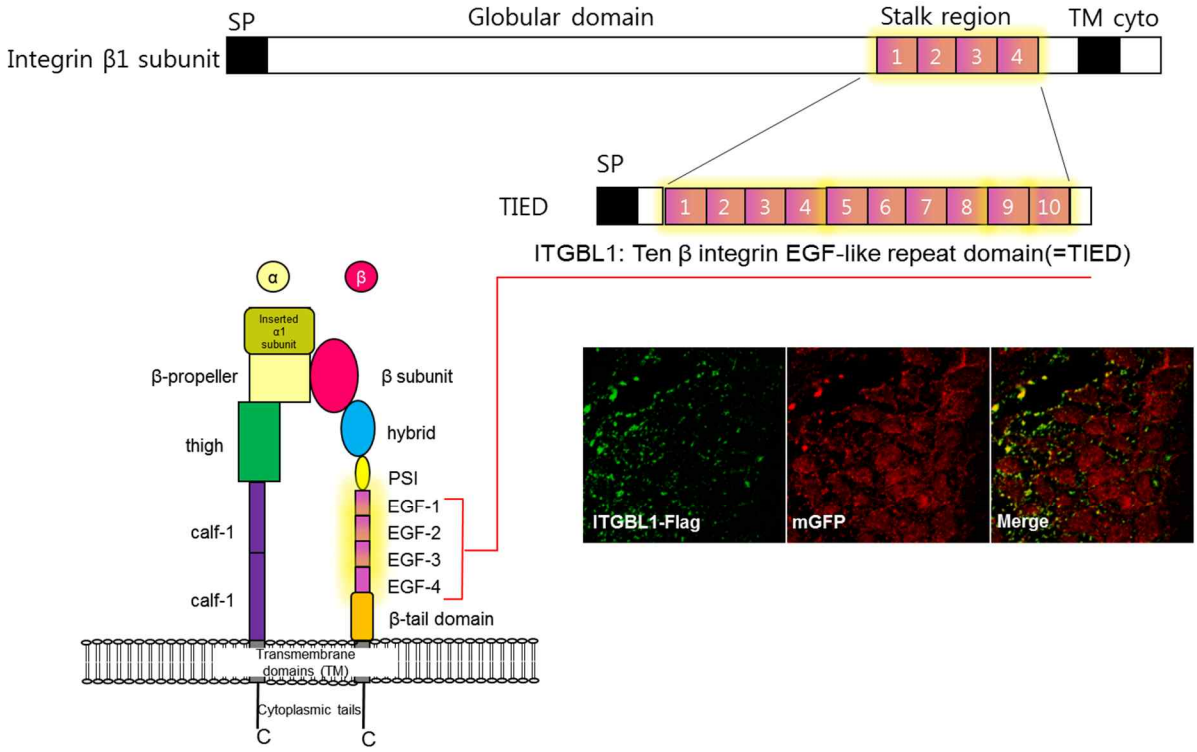

Figure 1-9. Structure of ITGBL1

The gene ITGBL1 is a β integrin-related extracellular matrix protein which was first cloned and characterized from an osteoblast cDNA library [40].

The ITGBL1 gene is composed of 10 domains and is called the EFG-like repeat domains by the secondary structure of the gene. This gene encodes a β integrin-related protein that is a member of the EFG-like protein family. The encoded protein contains integrin-like cysteine-rich repeats and a signal peptide for secretion. Alternative splicing results in multiple transcript variants. It has been reported that ITGBL1 is involved in cancer cell migration through TGF-β, Wnt/PCP, and focal adhesion kinase signaling in cancer cells. However, studies on the molecular function of ITGBL1 in the developmental stage have not yet been reported.

Chapter 2. ITGBL1 modulates integrin activity to promote cartilage formation and protect against arthritis

2-1. Introduction

Chondrocytes are responsible for the formation of cartilage-specific extracellular matrices (ECM), and ECM-driven signaling is critical for the pathophysiology of destructive cartilage disorders [41, 42]. ECM-chondrocyte interaction is mainly mediated by integrins, heterodimeric receptors for ECM molecules including fibronectin, collagen, and laminin. Chondrocytes express various subunits of integrin-α and integrin-β [41], Furthermore, the profile of integrin expression is dynamically regulated during chondrogenic differentiation [43, 44] and development of disease, such as osteoarthritis (OA) [45-48].

Recent research indicates that integrin-fibronectin interaction promotes the condensation of prechondrocytes [49-51] and is necessary for chondrogenic differentiation [52-56]. Other studies, however, reported that chondrogenic differentiation requires reduced integrin signaling [31], [57, 58]. Furthermore, several studies suggested that chondrogenesis is differentially regulated by integrins in a stage-dependent or context-dependent manner [59-61]. However, we do not understand how developing and mature chondrocytes dynamically regulate integrin signaling, which may exert negative effects on cartilage formation. Integrin signaling also mediates the catabolic reactions responsible for joint destruction in osteoarthritis (OA) development [62-65]. Fragmented ECM molecules such as fibronectins (Fn-fs) are known to trigger catabolic gene expression such as that of matrix metalloproteinase 3 (*Mmp3*), *Mmp13*, and *Adamts5* (*a disintegrin and metallopeptidase with thrombospondin type 1 motif 5; aggrecanase-2*), and to synergistically accelerate OA development. This Fn-fs-induced catabolic gene expression is mediated, in part, by integrins, although there are conflicting reports that integrins may not be involved in Fn-fs-mediated chondrolysis [66-68]. ITGBL1

was originally called "ten beta integrin EGF(Epidermal Growth Factor)-like repeat domains" due to its secondary structure [40]. A recent study implicated ITGBL1 in cancer cell migration via TGF-β, Wnt/PCP, and focal adhesion kinase (FAK)/Src signaling [69-71]. Additionally, ITGBL1 has been shown to be the key regulator of liver fibrosis [72]. However, the molecular functions of ITGBL1 in developing animals have not yet been examined.

Here, by performing unbiased transcriptome profiling, we found that developing chondrocytes secrete ITGBL1 to promote chondrogenesis. We show that ITGBL1 functions as an inhibitor of integrin-ECM interaction that is critical for both cartilage formation and OA development. ITGBL1 function is highly conserved in vertebrates, including *Xenopus laevis,* mouse, and human. *Itgbl1* expression was decreased in damaged articular chondrocytes from OA patients. Using a mouse model of surgically-induced OA, we show that ITGBL1 can protect against OA development in joint cartilage.

2-2. Material and methods

Xenopus embryo manipulation

Adult female frogs were induced to ovulate by injection of human chorionic gonadotropin, and eggs were fertilized in vitro and dejellied in 3 % cysteine (pH 7.9) in 1/3× Marc's Modified Ringer's (MMR) solution. Fertilized eggs were grown in 1/3× MMR. Animals were obtained from the Korean *Xenopus* Resource Center for Research. Adult *Xenopus laevis* were housed under a 12-h light/dark cycle at 18°C in containers according to the guidance of the Animal Care and Use Committee of the Institutional Review Board of UNIST. We designed splice-blocking antisense morpholino for *Itgbl1* based on sequences from the Xenbase database. We obtained *Itgbl1*-MO (AGTAGGGAAGATATACAGACCTGCA) from Gene Tools.

Cell culture

Human PC3 cells (ATCC), HEK293T cells (ATCC), or hBMSCs (ATCC) were cultured in 1 % L-glutamine, 10 % fetal bovine serum (FBS), 1 % penicillin-streptomycin, RPMI 1640 medium, Dulbecco's Modified Eagle Medium (DMEM, Sigma), and α-MEM (Sigma). To assess chondrogenesis of hBMSCs, we employed pellet, micromass, or Transwell culture systems.

Articular chondrocytes were isolated from femoral condyles and tibial plateaus of postnatal day 5 mice. Cartilage tissues were digested with 0.2 % collagenase type II. Chondrocytes were maintained in DMEM containing 10 % FBS and penicillin and streptomycin. Cells on culture day 3 used for further treatments.

We purchased human chondrocytes from Cell Application, Inc. According to the manufactures datasheet, the chondrocytes were isolated from the human fetal femoral cartilages of a single donor female at 20 weeks gestation. Human bone-marrow stem cells were purchased from the ATCC.

Micromass cultures of mesenchymal cells were prepared as described previously. Mesenchymal cells obtained from E11.5 embryos of ICR mice were digested with 1 % trypsin and 0.2 % type II collagenase and maintained to induced chondrogenesis and hypertrophic maturation. A total of 2×10^7 cells/ml was suspended in DMEM/F-12 medium (1:1) containing 10 % (v/v) FBS. The cells were spotted as 15 μl drops on culture dishes and maintained for 6 days to induce chondrogenesis. Chondrogenesis was confirmed by Alcian blue staining of sulfated proteoglycans.

Integrin activation and inactivation

To activate integrin, we used Mn^{2+} and DTT (BIOSESANG). After harvesting, the cells were resuspended in medium containing 5 mM DTT and incubated for 30 minutes. The cells were then centrifuged for 5 min at 70×g, floating cells were removed, and the remaining cells were cultured on a cover slip coated with fibronectin. The cells on the cover slip were incubated for 4 hours at 36 °C and fixed for image analysis. In the case of Mn^{2+}, 0.07 mM or the indicated concentration of $MnCl_2$ was included in the medium. Cells were treated with integrin inhibitor BIO1211, obtustatin, or ATN-161 (TOCRIS) and incubated at 36 °C for 12 hours followed by harvesting for RNA extraction.

Adenoviral infection and biochemical analysis

Adenovirus carrying mouse *Itgbl1 (BC020152)* (Ad-*Itgbl1*) or shRNA targeting mouse *Itgbl1* (Ad-*Itgbl1* shRNA), eGFP (Ad-eGFP), and empty virus particles (Ad-C) were purchased from Vector Biolabs. Articular chondrocytes were isolated from knee cartilage of mice on postnatal day 5 mice. On day 2 of culture, chondrocytes were treated with IL-1β or infected with Ad-*Itgbl1* at the indicated multiplicity of infection. *Itgbl1* was detected by RT-PCR and measured by quantitative PCR with specific primers (human *ITGBL1*, sense: 5'-TCATCTGCTCTAATGCAGGTACA-3', antisense: 5'-CGGATCAACATCGTGACAGGTA-3'; mouse *Itgbl1*, sense: 5'-GCAGAGTCCGAACGCAGAT-3', antisense: 5'-ACACAGTGGACCGAAGTAGGT-3; Mouse *FAK* sense: 5`-GTGGCCTGCTATGGATTTCG-3`, antisense: 5`-TTGCATGTAGTCACTCTTCACC-3`). *Col2a1* expression in hBMSCs was detected by quantitative PCR with specific primers (sense: 5'- GGACTTTTCTCCCCTCTCT -3', antisense: 5'- GCCCGAAGGTCTTACAGGA-3'). Other primer sequences for amplifying target genes were as previously described [73].

Ad-*Itgbl1* was used to overexpress ITGBL1 in mesenchymal cells in micromass culture. Mesenchymal cells were maintained as micromass culture for 10 hours and infected for 1 hour with Ad-*Itgbl1*. Infected cells were cultured for up to 6 days in serum-free medium. Chondrogenesis was determined by Alcian blue staining.

Human OA cartilage and mouse model of OA

Human cartilage samples were obtained from individuals 45–65 years of age undergoing total knee arthroplasty after obtaining written informed consent as approved by the Institutional Review Board of the Catholic University of Korea (UC14CNSI0150). Mouse experiments were approved by the Animal Care and Use Committee of the Ajou University College of

Medicine. Male C57BL/6 mice (10-week old; DBL Co., Ltd., Chungbuk, Korea) were housed (n=4 per cage) under controlled temperature (23 °C) and were exposed to a 12-hour light/dark cycle. Food and water were provided *ad libitum*.

For the intra-articular depletion of ITGBL1 in Fig. 7, we performed intra-articular injections (every 3 days for 3 weeks) of Ad-*Itgbl1* shRNA (1×10^9 pfu in a total volume of 10 μl) or ATN-161. The experiment was repeated a total of five times independently with two mice per experimental condition in each independent test. However, one mouse was lost due to unforeseen circumstances during the experiment, and so the total number of mice were nine (n=9). Mice were sacrificed 3 weeks after the first intra-articular injection.

For the DMM experiment in Fig. 8, we performed intra-articular injections of Ad-*Itgbl1* (1×10^9 pfu in a total volume of 10 μl) as previously described [74]. The experiment was repeated a total of six times independently with two mice per experimental condition in each independent test, and so the total number of mice were twelve (n=12). Ten weeks after DMM surgery, mice were sacrificed. For rescue experiments, intra-articular injection was initiated 5 weeks after DMM surgery and performed once per week for 6 weeks. Decalcified cartilage was stained with Safranin O and scored using the OARSI grading system. Synovitis was determined by Safranin O and hematoxylin staining, and synovial inflammation (grade 0–3) was scored as described previously [73] quantified as described previously [74]. Subchondral bone sclerosis was determined by measuring the thickness of the subchondral bone plate [75]. Osteophyte development was identified by Safranin-O staining, and osteophyte maturity was determined by measuring the thickness of the subchondral bone plate [76].

Statistical analysis

Data based on an ordinal grading system, such as OARSI grade, were analyzed using non-parametric statistical tests. All values are expressed as mean ± standard error of the mean (SEM) and were subjected to Student's *t*-test for pairwise comparisons or one-way analysis of variance (ANOVA) for multiple comparisons using the SPSS v. 10.1 statistical package or Prism.

2-3. Results

Itgbl1 promotes facial cartilage formation in the *Xenopus* embryo.

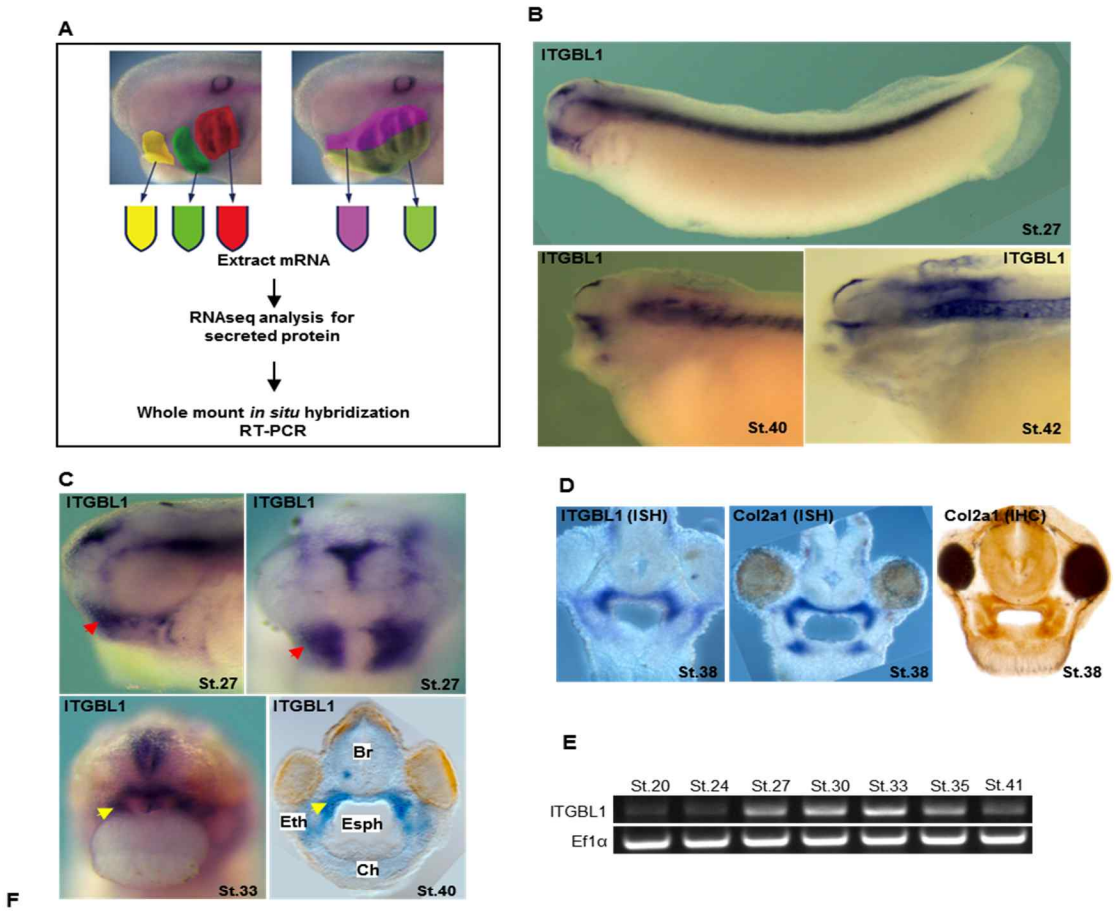

Figure 2-1-1. ITGBL1 expression pattern in facial cartilage tissues and homology of ITGBL1 across vertebrates.

A. The transcriptome of developing pharyngeal arches dissected from *Xenopus* embryos was analyzed by RNA-seq. The colors indicate dissected tissues from the pharyngeal arches. **B.** ITGBL1 expression was analyzed by whole-mount *in situ* hybridization (WISH). **C**. ITGBL1 expression in developing pharyngeal arches and facial cartilages was analyzed by RNA *in situ* hybridization in sectioned embryonic samples (Br, brain; Eth, ethmoidal plate; Esph, esophagus; Ch, Ceratohyal cartilage). **D.** ITGBL1 expression compared to the Col2a1-positive prechondrogenic facial tissues. Sibling embryos were sectioned and processed for RNA WISH using antisense probes for ITGBL1 or Col2a1. Immunohistochemistry was performed using anti-Col2a1 antibody. **E.** RT-PCR assay showing ITGBL1 expression during specific chondrogenesis stages in developing embryos. **F.** The homology of ITGBL1 amino acid sequences across vertebrates.

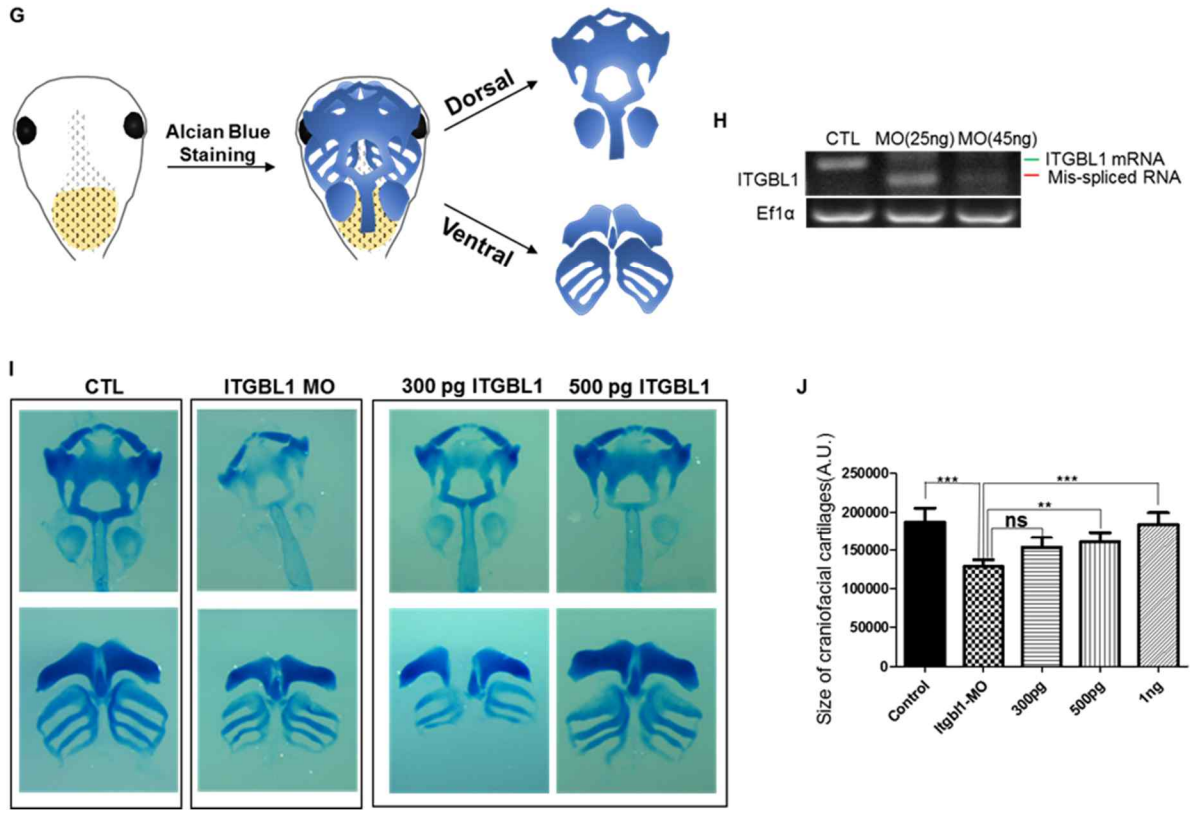

Figure 2-1-2. ITGBL1 promotes facial cartilages formation in the *Xenopus embryo*.

G. Cartilage separation pattern of *Xenopus laevis*. H. Morpholino efficiency is shown by agarose gel.

I. Alcian blue-stained images of craniofacial cartilages in control, ITGBL1-depleted (MO, morpholino), and ITGBL1 -rescued embryos. Scale bars: 500um. **J.** Quantification of facial craniofacial cartilages in (**I**). n: Control=33, ITGBL1-MO=42, ITGBL1-MO+300pg=31, ITGBL1-MO+500pg=38, ITGBL1-MO+1000pg=38.

Pharyngeal arches of vertebrate embryos develop to form various facial tissues including cartilage, bone, muscle, and other connective tissues [77]. The pharyngeal arches of the *Xenopus* embryo provide accessible and tractable tissues to study the interplay among various tissues during cartilage formation [78, 79]. Therefore, we used *Xenopus* pharyngeal arches to perform an unbiased transcriptomics search to discover potential therapeutic targets

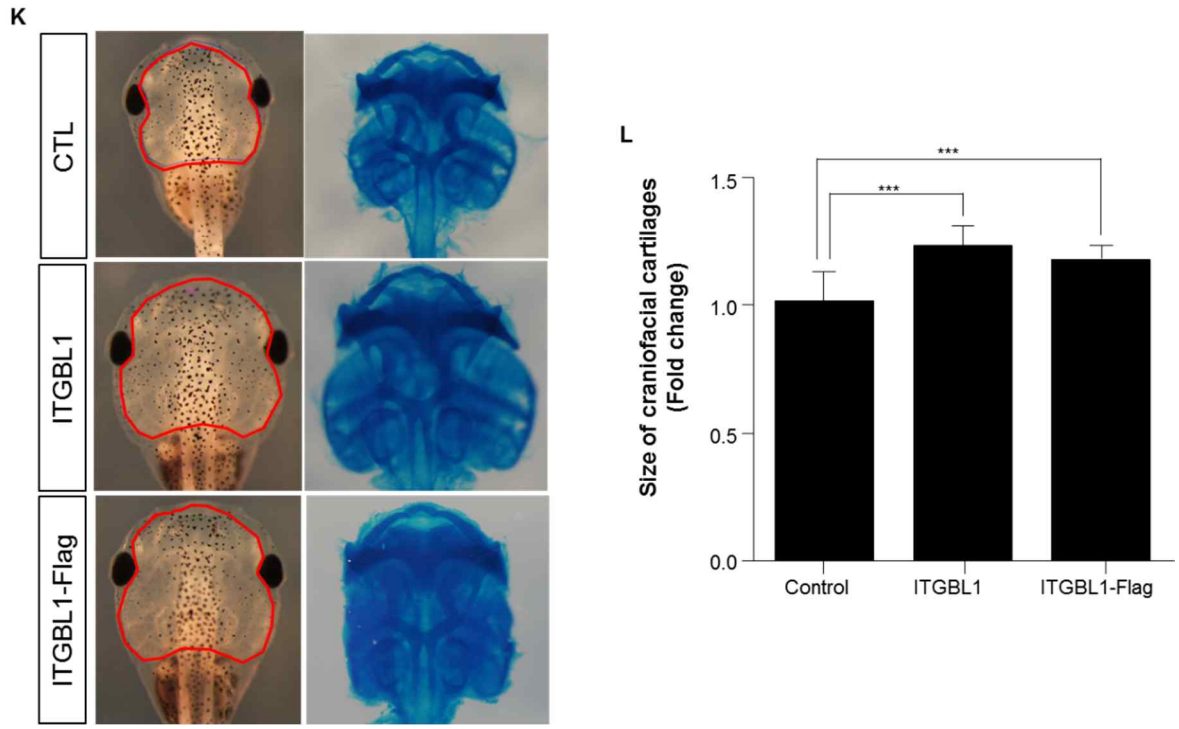

Figure 2-1-2. ITGBL1 promotes facial cartilages formation in the *Xenopus embryo*.

K. Alcian blue-stained images of craniofacial cartilages of control and ITGBL1-overexpressing embryos. **F.** Quantification of facial cartilages in L. n: Control=17, ITGBL1=17, ITGBL1-Flag+300pg=17.

in secreted proteins involved in cartilage formation. We dissected each pharyngeal arch and analyzed gene expression profiles by performing RNAseq experiments. Subsequently, we searched for secreted proteins differentially expressed in pharyngeal arches (Table1). Among hundreds of differentially expressed secreted proteins, whole-mount in situ hybridization (WISH) and reverse transcription polymerase chain reaction (RT-PCR) analyses revealed that *Itgbl1* is predominantly and temporally expressed in chondrogenic precartilage tissues (Fig. 2-1-1B-E). ITGBL1 is highly conserved among vertebrates (Fig. 2-1-1F). Recent studies on the function of ITGBL1 implicated it in cancer cell metastasis and cell migration. However, *Itgbl1*

expression profiles and functions in developing vertebrate embryos have not been previously examined.

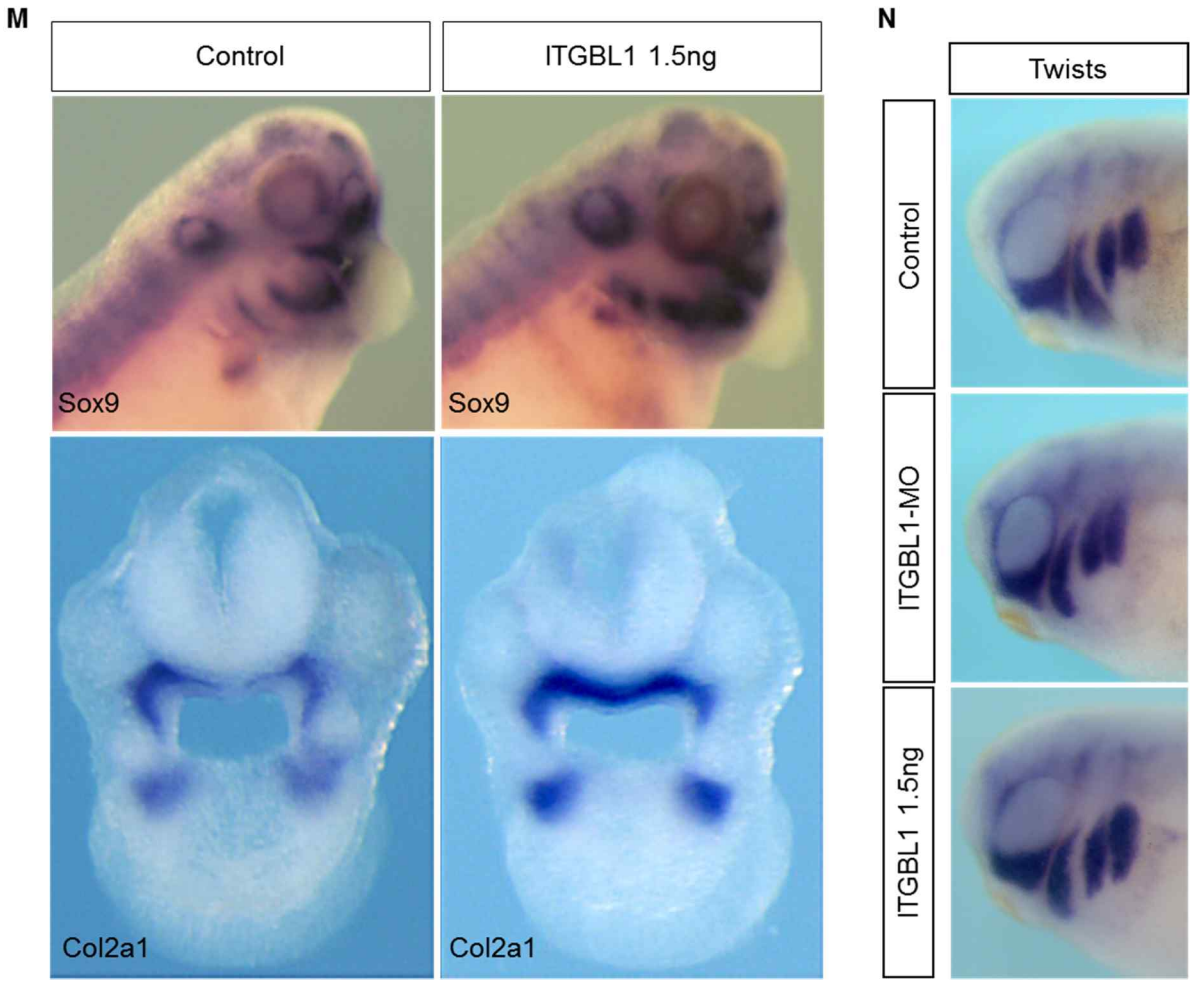

Figure 2-1-3. ITGBL1 promotes facial cartilages formation in the *Xenopus embryo*

M. Expression of Sox9 and Col2a1 in control and ITGBL1-overexpressing embryos. **N.** Neural crest-cell migration as analyzed by Twist expression. Scale bars: 500um

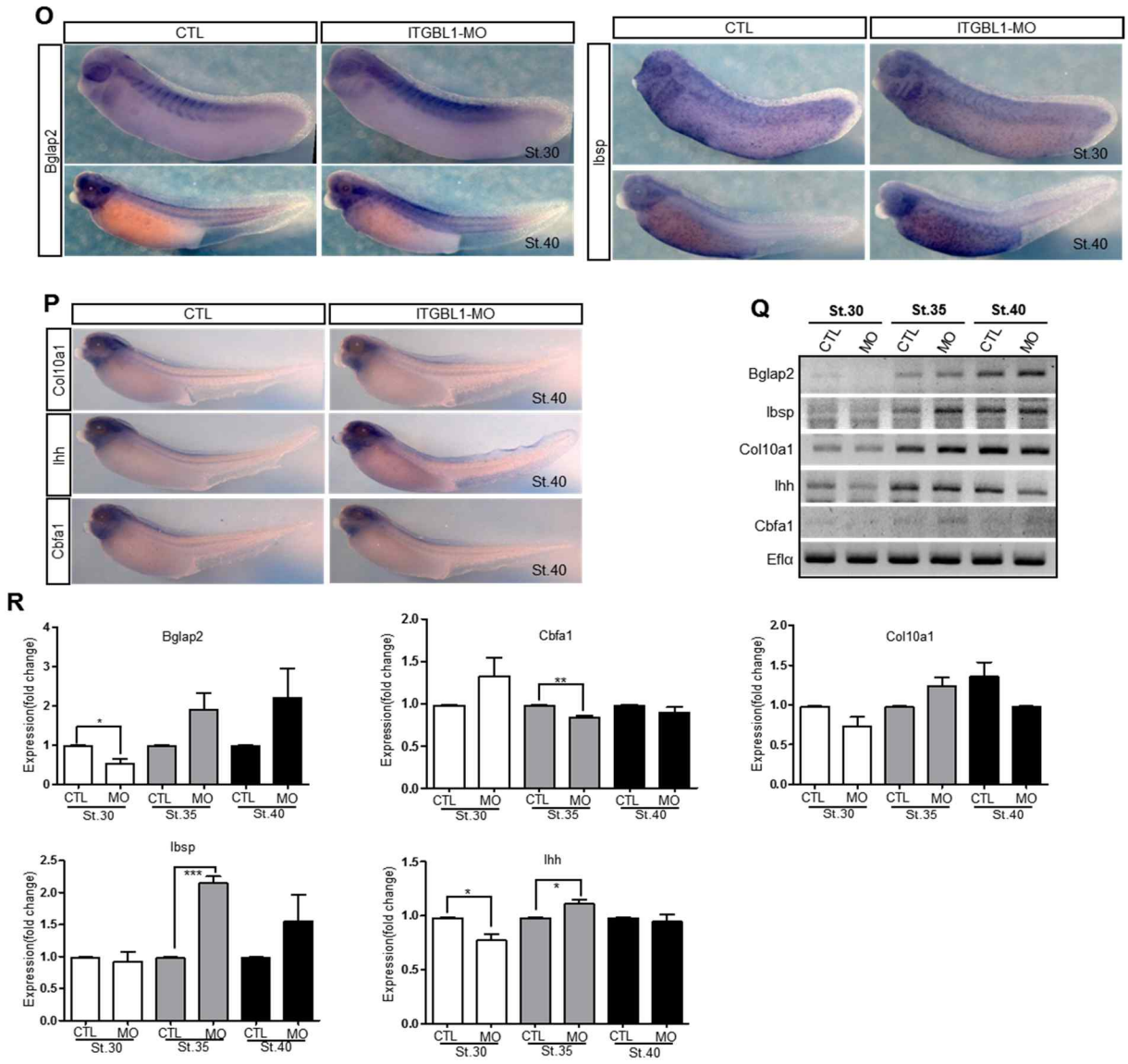

Figure 2-1-4. Neural crest-cell migration, hypertrophic chondrocyte development, and osteogenic differentiation after ITGBL1 depletion.

O-P. Osteogenic differentiation (**O**) and hypertrophic chondrocyte development (**P**) analyzed by RNA WISH. **Q.** RT-PCR analysis after ITGBL1 depletion. **R.** The gene expression shown in (**Q**) was quantified by q-PCR and plotted.

To examine whether ITGBL1 is involved in cartilage development, we knocked down *Itgbl1* expression using a splice-blocking morpholino oligo (*Itgbl1*-MO) in *Xenopus laevis* embryos. *Itgbl1*-MO injection effectively inhibited the formation of mature *Itgbl1* mRNA (Fig. 2-1-2H).

Alcian blue staining revealed severely hypoplastic craniofacial cartilages in *Itgbl1*-MO injected embryos that were rescued by co-injection of *Itgbl1* mRNA (Fig. 2-1-2I, J), suggesting that cartilage malformation is a specific phenotype of loss of *Itgbl1* expression. By contrast, *Itgbl1* overexpression via wild-type or C-terminal FLAG-tag fusion proteins increased the overall size of craniofacial cartilages significantly ($p<0.0001$) (Fig. 2-1-3K, L) and elevated expression of chondrogenesis markers, such as *Sox9* (*Sex-Determining Region Y-Box 9 Protein*) and *Col2a1(collagen, type II, alpha 1)* (Fig. 2-1-3M). Most craniofacial cartilage originates from cranial neural crest cells, which migrate into the pharyngeal arches and condense to form prechondrocytes [80]. We found that cranial neural crest cells migrated normally in *Itgbl1*-MO-injected embryos (Fig. 2-1-3N). We further assessed the late chondrogenic markers and bone formation in ITGBL1-depleted embryos. We observed that *Col10a1* (*collagen, type X, alpha 1*) and *Ihh* (*Indian hedgehog*) expression was slightly reduced at Stage 40, when chondrogenesis starts and cartilages form in the *Itgbl1* morphant embryos (Fig. 2-1-4O-R). We also observed slightly increased expression of *Bglap2* (*bone gamma-carboxyglutamate protein 2*) and *Ibsp* (*integrin binding sialoprotein*) in the *Itgbl1* morphant embryos (Fig. 2-1-4O-R).

Taken together with our observation that *Itgbl1* expression in normal embryos is strongest after neural crest cell migration (Fig. 2-1-1E), this finding suggests that *Itgbl1* contributes to craniofacial cartilage formation after the migration of neural crest cells.

ITGBL1 depletion inhibits cartilage-specific ECM deposition.

Next, we monitored the chondrogenic process in ITGBL1-depleted embryos by injecting *Itgbl1*-MO unilaterally in two-cell-stage embryos (Fig. 2-1-5O) and visualizing chondrogenic tissue using an anti-COL2A1 antibody (Fig. 2-1-4J). Cartilage-specific COL2A1 expression was sharply reduced in *Itgbl1*-MO-injected tissue (Fig. 2-1-4J), but there were no changes in fibronectin deposition (Fig. 2-1-6S), suggesting that ITGBL1 depletion mainly

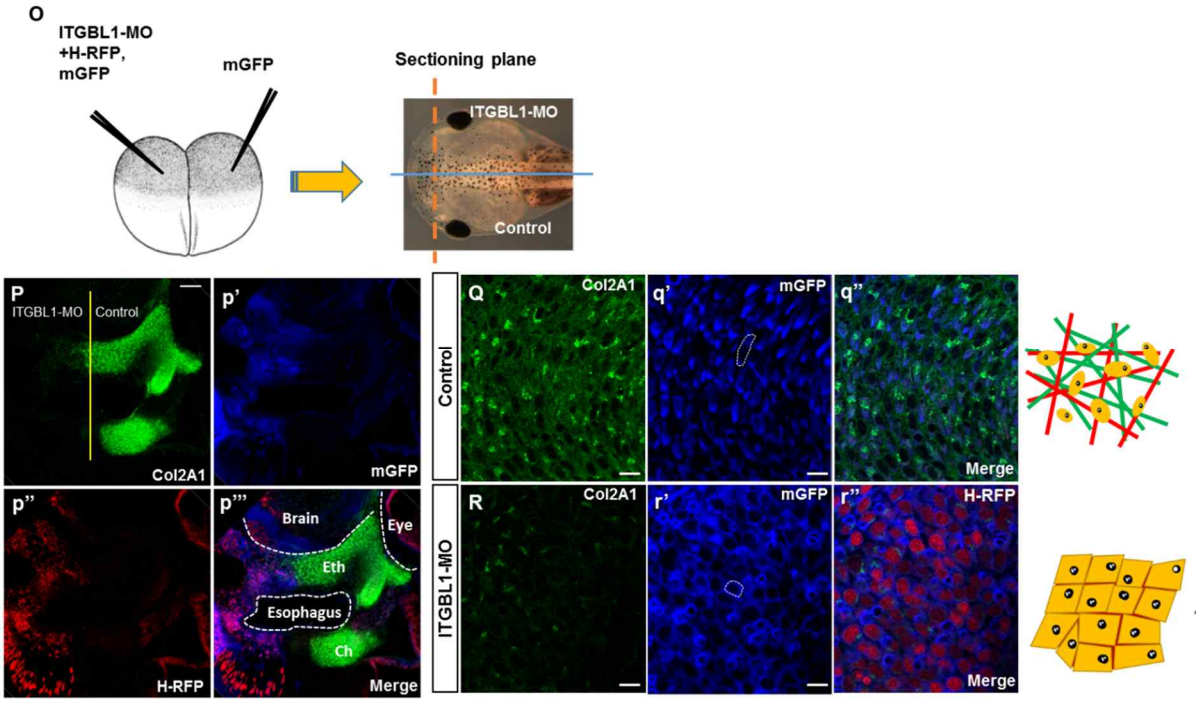

Figure 2-1-5. ITGBL1 depletion inhibits cartilage-specific ECM deposition.

O. Schematic illustrating ITGBL1 unilateral injection [contralateral region injected with mGFP (membrane-green fluorescent protein)] into two-cell-stage *Xenopus* embryos to examine the ITGBL1 loss-of-function phenotype in a mosaic animal. **P.** Immunostaining for Col2a1 (green) in facial cartilages in bilaterally njected embryos (50um sections). **p'.** mGFP pseudo-colored blue. Histone-red fluorescent protein (H-RFP, **p''**, **p'''**) was co-injected as a tracer. Scale bars: 100 μm. **Q-R.** High-magnification images of the ethmoidal plate (Eth in **p'''**) in control and Itgbl1-MO-injected embryos.

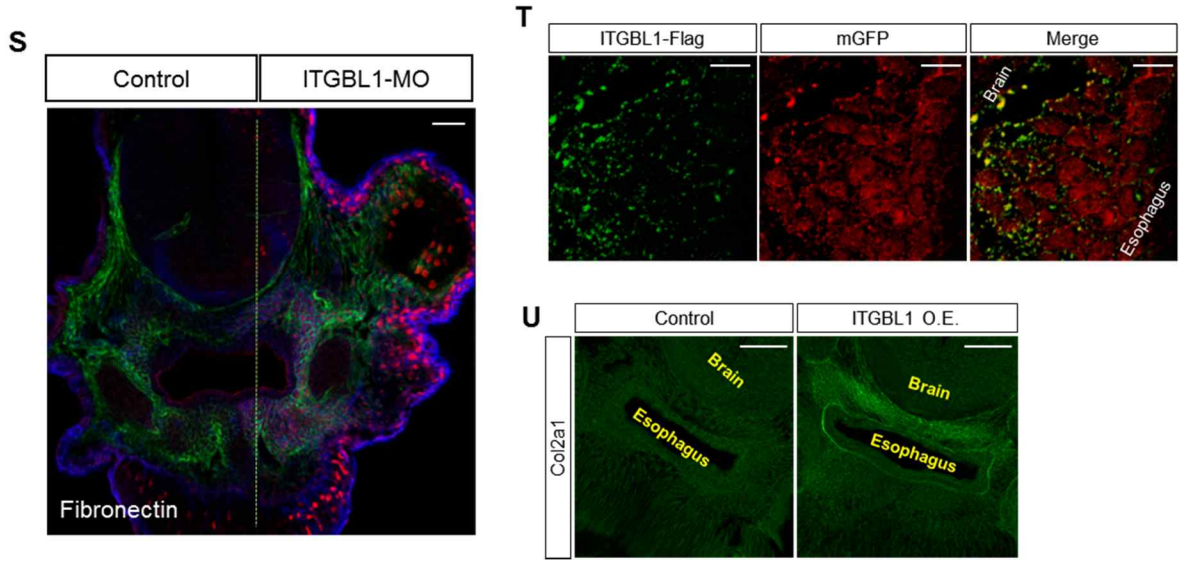

Figure 2-1-6. ITGBL1 depletion inhibits cartilage-specific ECM deposition.

S. Fibronectin deposition in facial tissue was visualized by immunostaining after unilateral injection of Itgbl1-MO. Histone-RFP (H-RFP) was co-injected as a tracer. Scale bars: 100μm. **T.** ITGBL1-FLAG fusion proteins expressed in craniofacial prechondrocytes. Immuno-fluorescent staining was performed with anti-FLAG antibody (Green). mGFP was pseudo-colored as red. Scale bars: 20 μm. **U.** Control and ITGBL1-overexpressing *Xenopus* embryo (stage 37) sections stained for Col2a1 (Green). Scale bars: 500 μm. Data are shown as mean ± SEM (** $p<0.005$, *** $p<0.0005$).

affects cartilage-specific ECM deposition. ITGBL1 knockdown also caused abnormal prechondrocyte morphology. The chondrogenic process in facial cartilage begins with the condensation of migratory cranial neural crest cells. Then prechondrocytes secrete cartilage-specific ECM molecules, while changing their morphology into oval-shaped mature chondrocytes. Unilateral depletion of ITGBL1 resulted in stark differences in cell morphology and ECM secretion. Control chondrocytes secreted cartilage-specific ECM and were well dispersed with a typical oval shape (Fig. 2-1-5Q). However, ITGBL1-depleted cells failed to secrete ECM and maintained tight contact with neighboring cells (Fig. 2-1-5R), suggesting that

chondrogenesis was halted at the condensation stage. We also examined ITGBL1 localization in prechondrocytes by expressing FLAG-tagged ITGBL1 in *Xenopus* embryos. ITGBL1-FLAG localized to the cell periphery as puncta (Fig. 2-1-6T). Furthermore, ectopic expression of ITGBL1 in embryonic prechondrocytes promoted chondrogenic ECM deposition earlier than in control prechondrocytes (Fig. 2-1-6U).

ITGBL1 function is necessary for chondrogenic differentiation of human BMSCs.

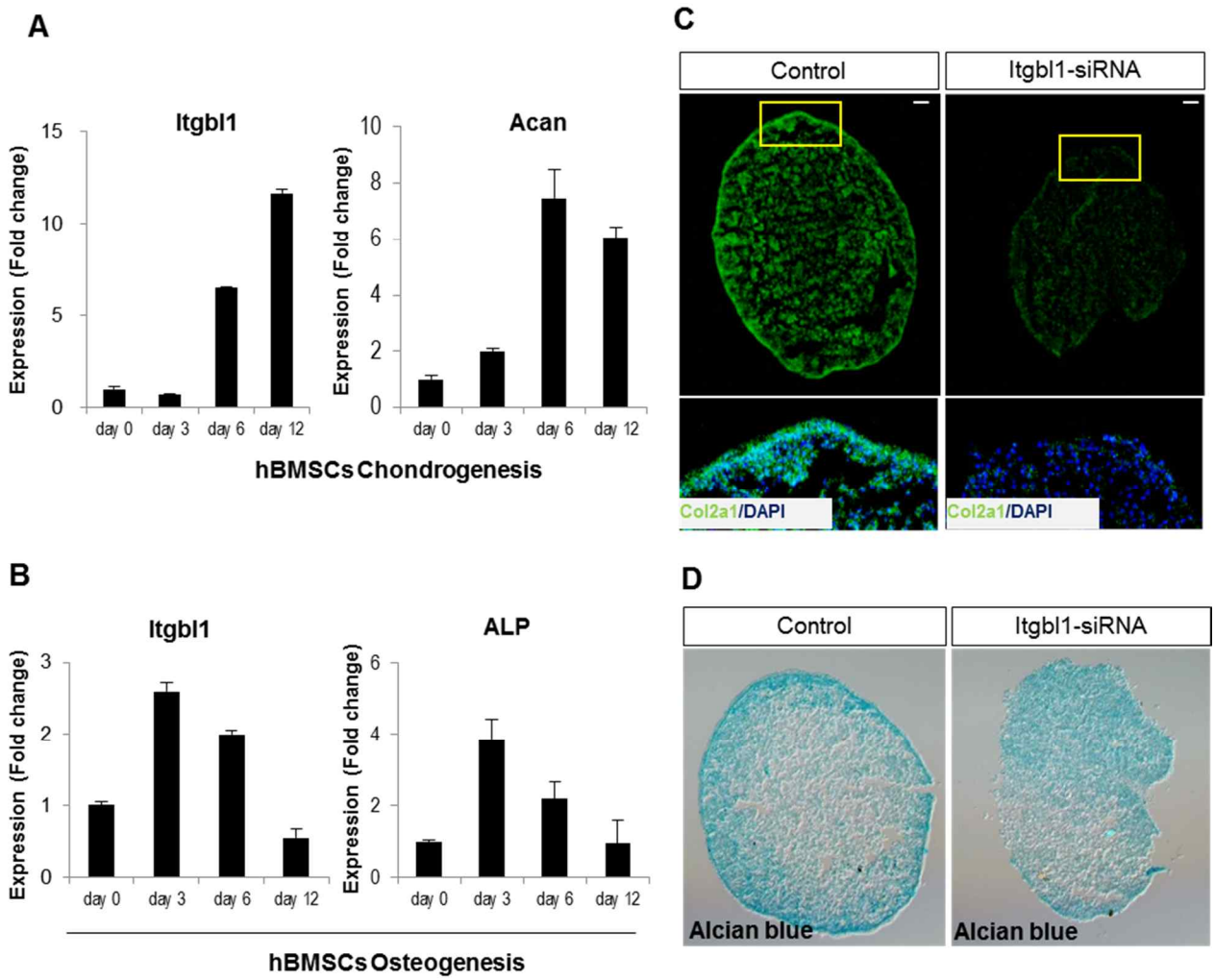

Figure 2-2-1. ITGBL1 function in chondrogenic differentiation of human bone-marrow stem cells (BMSCs) and mouse limb-bud mesenchymes.

A. ITGBL1 and aggrecan (Acan) expression quantified by q-PCR analysis during chondrogenesis. **B.** ITGBL1 and alkaline phosphatase (ALP) expression quantified by q-PCR analysis during osteogenesis. **C, D.** Frozen sections (10 μm) of control or ITGBL1-depleted hBMSC-derived chondrogenic pellets stained with anti-Col2a1 antibody (**C**) or Alcian blue (**D**). Scale bars: 100 μm.

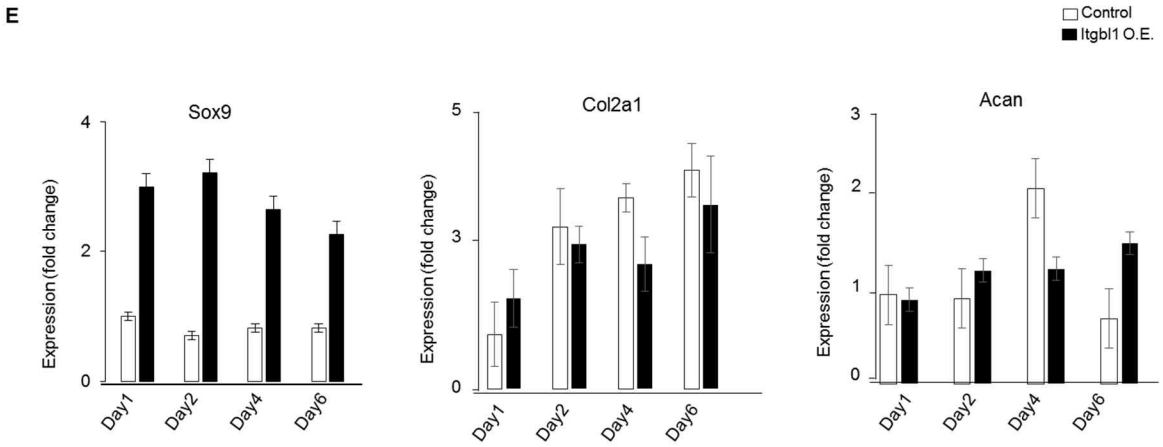

Figure 2-2-2. ITGBL1 is not an instructive signal to promote chondrogenesis without chondrogenic inducer from hBMSC.

E. Chondrogenic gene expression in hBMSCs after ITGBL1 overexpression.

Having exploited the in vivo capabilities of the *Xenopus* embryo to identify a novel regulator of cartilage development, we next sought to explore its mechanism of action in chondrogenic differentiation of hBMSCs (bone marrow-derived mesenchymal stem cells). RT-PCR experiments revealed that *Itgbl1* expression in chondrogenic hBMSCs gradually increased and reached a peak on day 12 of differentiation (Fig. 2-2-1A), whereas *Itgbl1* expression had decreased by this time point in osteogenic hBMSCs (Fig. 2-2-1B). When we carried out siRNA-mediated *Itgbl1* knockdown and induced chondrogenesis in hBMSCs, *Itgbl1* expression was effectively decreased, although it was gradually restored by day 5 (fig. S4A-B). Alcian blue and COL2A1 immunostaining showed that control hBMSC pellets deposited chondrogenic ECM normally, whereas *Itgbl1* knockdown reduced chondrogenic ECM and COL2A1 expression (Fig. 2-2-1C-D). We further tested whether *Itgbl1* overexpression promotes chondrogenesis in a non-chondrogenic condition. *Itgbl1* overexpression increased *Sox9* expression without chondrogenic inducers such as TGF-β (Fig. 2-2-2E). However,

expression of other chondrogenic genes, such as *Col2a1 and Acan (Aggrecan)* were not consistently sustained in *Itgbl1*-overexpressing hBMSCs (Fig. 2-2-2E). Because *Itgbl1* overexpression promoted chondrogenic differentiation in embryonic cartilage tissue, and not

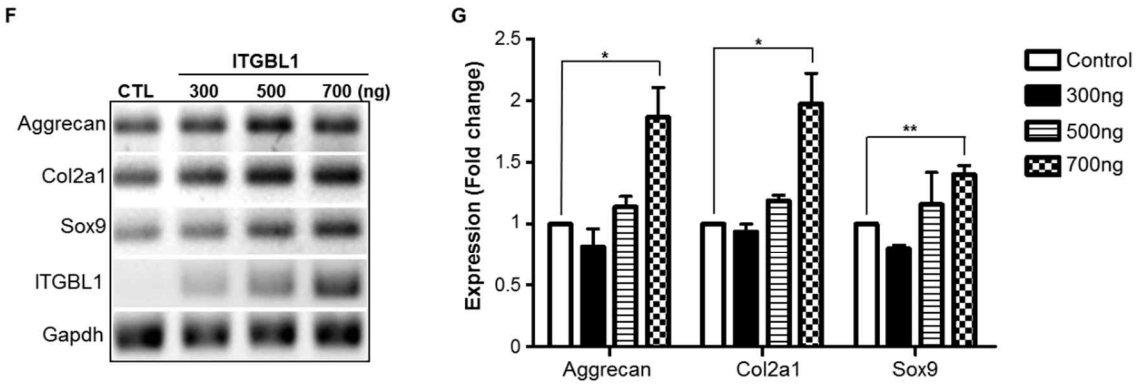

Figure 2-2-3. ITGBL1 function is necessary for chondrogenic differentiation of mouse chondrocyte.

F. Chondrogenic gene expression upon ITGBL1 overexpression with increasing doses in the absence of differentiation medium analyzed by RT-PCR. (**F**) Chondrogenic gene expression Sown in (**G**) quantified by q-PCR. **G**: data are shown as mean ± SEM from three biological replicate experiments.

in hBMSCs, we reasoned that ITGBL1 may need other specification signals to promote chondrogenesis. We tested ITGBL1 function in promoting chondrogenesis in the ATDC5 cell line and mouse chondrogenic mesenchymes isolated from limb buds, because these cells are already specified to differentiate into chondrocytes. Indeed, *Itgbl1* overexpression consistently promoted chondrogenesis in ATDC5 cells (Fig. 2-2-2F, G and fig. S5B) and in limb-bud mesenchyme (data not show). Furthermore, *Itgbl1* expression in chondrogenic ATDC5 cells prevented *Col10a1* expression, which suggests that hypertrophic differentiation is suppressed by ITGBL1 (fig. S5F, G). These results suggest that ITGBL1 enhances chondrogenesis and that the function of ITGBL1 is well conserved across vertebrates, including humans, although it may not be a master regulator of chondrogenic differentiation.

ITGBL1 inhibits integrin-ECM interactions.

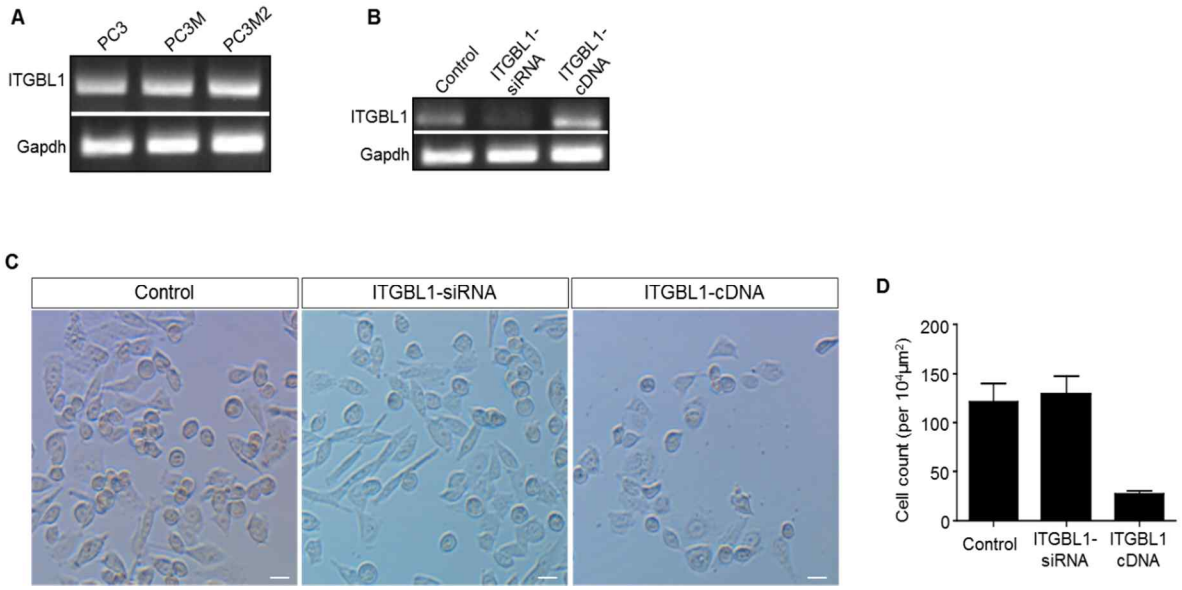

Figure 2-3-1. ITGBL1 reduces cell-ECM adhesion.

A. PC3 prostate cancer cells highly expressed ITGBL1. **B.** siRNA transfection decreased ITGBL1 expression in PC3 cells. **C-D.** Ectopic expression of ITGBL1 inhibited cell attachment to collagen-coated plates.

Cartilage phenotypes in *Itgbl1* morphants suggested that ITGBL1 may be necessary to progress past the condensation stage of chondrogenesis (Fig 1I). Prechondrocyte condensation is mainly mediated by integrin-fibronectin interaction [49-51]. However, integrin-mediated outside - in signaling needs to be inhibited for during chondrogenic differentiation [31, 57, 58]. Furthermore, increased FAK signaling negatively regulates cartilage formation [81]. These seemingly conflicting observations may be explained by the timing of integrin-ECM interaction, as integrin signaling may serve distinct roles at different stages of chondrogenesis [59-61]. Whereas early integrin-ECM interaction may be required to promote prechondrocyte

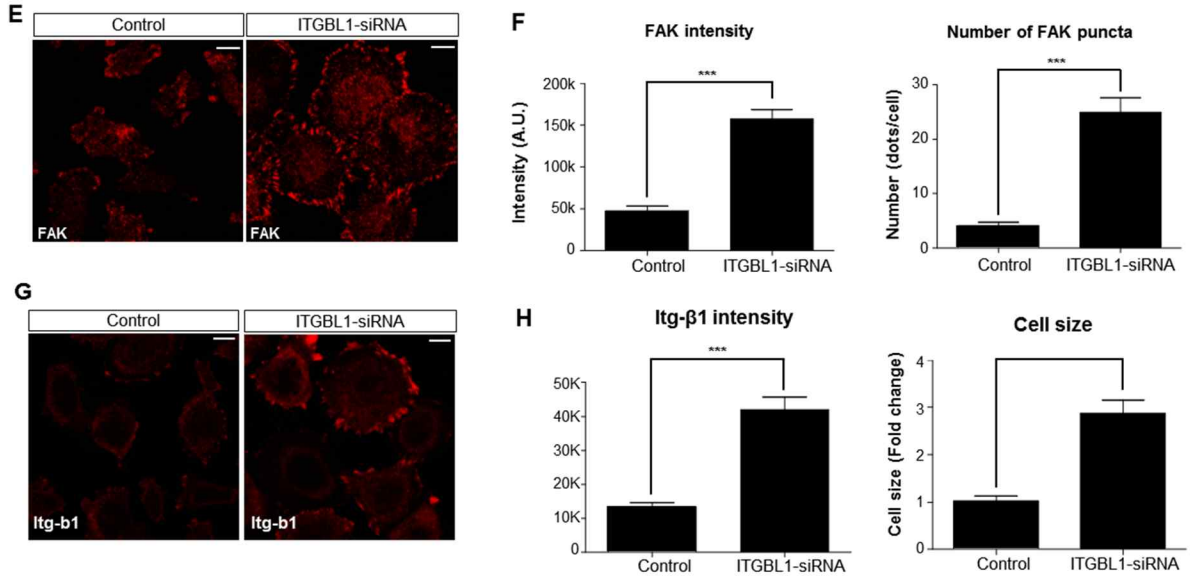

Figure 2-3-2. ITGBL1 inhibits active integrin-ECM complex formation

E. Immunofluorescent staining of FAK-positive focal adhesion complexes in control or ITGBL1-depleted PC3 cells. **F.** The expression intensity and number of FAK-positive focal adhesion (FA) complexes in (E). **n**: Control (CTL)=18, Itgbl1-siRNA=21. **G.** Immunofluorescent staining of integrin-β1-positive FA complexes in control and ITGBL1-depleted PC3 cells. **H**. The intensity of integrin-β1 expression and the size of the cells in (**G**). Scale bars: 10 μm (*** $p<0.0005$).

condensation, prechondrocyte-ECM interactions need to be inhibited for further ECM molecule secretion and changes in cell shape to occur during chondrogenesis. We then speculated that ITGBL1 might inhibit integrin-ECM interactions to decrease integrin-mediated outside-in signaling and to facilitate chondrogenesis after prechondrocyte condensation. In this situation, ITGBL1 may function as an integrin inhibitor. We predicted that siRNA-mediated ITGBL1 depletion would affect integrin-mediated cell behaviors, such as cell spreading and binding to the ECM-coated plates. To test this hypothesis, we used siRNA to transfect PC3 human prostate cancer cells, which express *Itgbl1* at a high level (Fig. 2-3-1A, B). As expected, ITGBL1 depletion increased cell size, whereas *Itgbl1* overexpression caused cells to detach from collagen-coated plates (Fig. 2-3-2E, F).

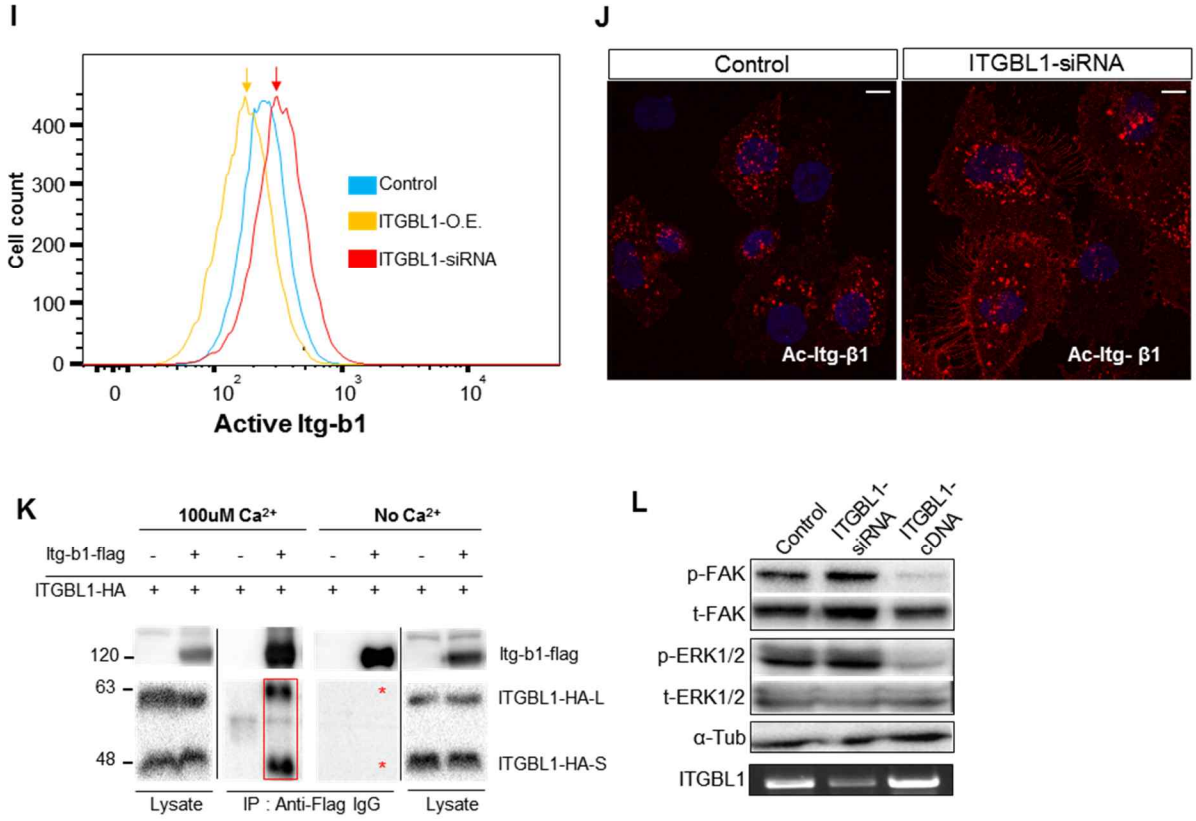

Figure 2-3-3. ITGBL1 inhibits integrin-ECM complex formation in PC3 cells.

I. FACS analysis using active integrin-β1-specific antibodies (HUTS-4) in control, ITGBL1-depleted, or ITGBL1-overexpressing PC3 cells. **J.** Active integrin-β1-specific antibody staining in control or ITGBL1-depleted PC3 cells. **K.** Co-immunoprecipitation of ITGBL1-HA and integrin-β-Flag in the presence or absence of Ca^{2+}. Transfection of C-terminal HA-tag fusion construct of ITGBL1 yielded two major products of 63 kDa and 48 kDa, which were ITGBL1-L and ITGBL1-S, respectively. **L.** ITGBL1 overexpression inhibited FAK and ERK 1/2 phosphorylation. Data are shown as mean ± SEM.

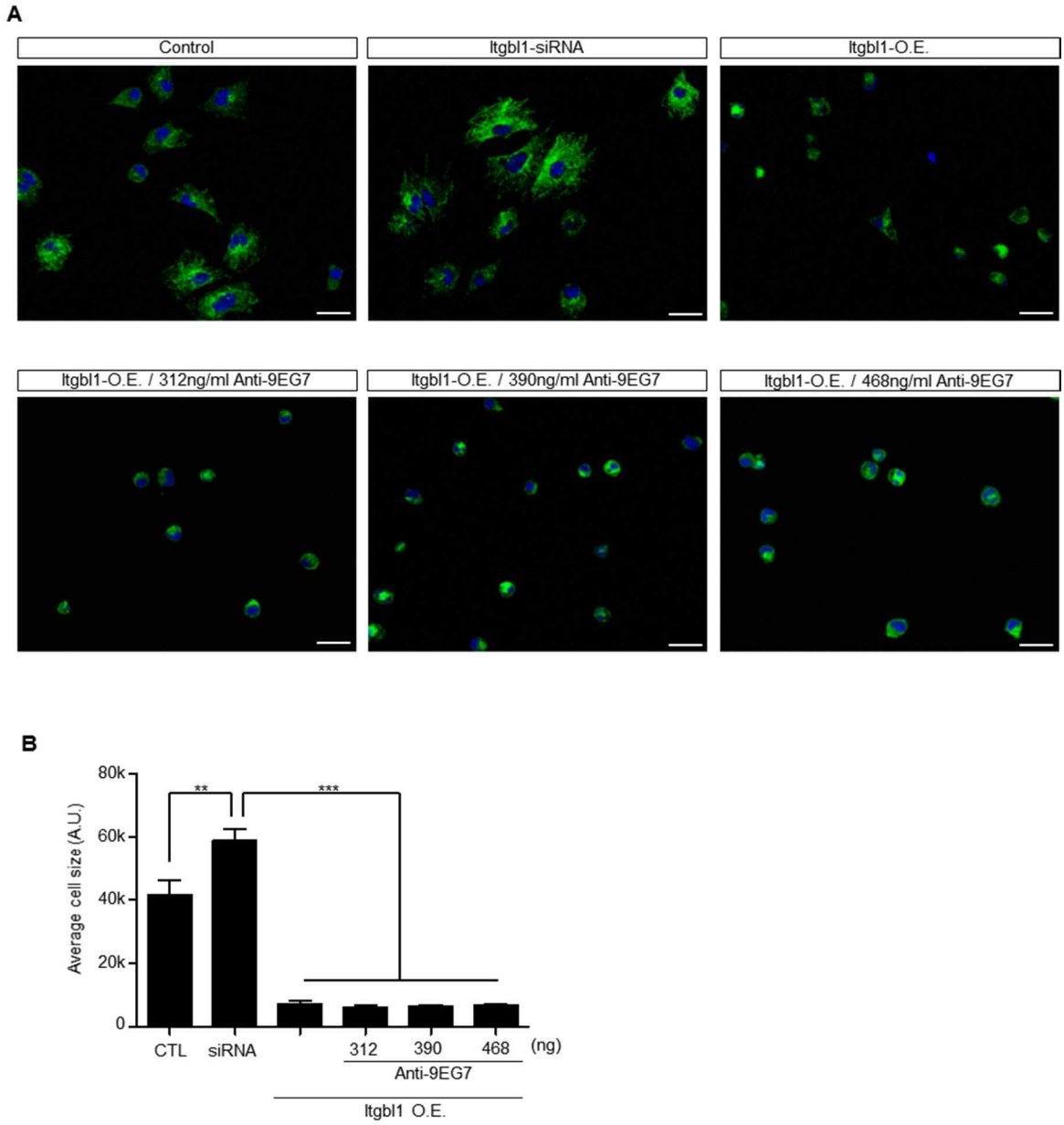

Figure 2-4-1. ITGBL1-induced integrin inactivation is not recovered by integrin-activating antibody.

A-B. Cell adhesion and spreading were analyzed in control, ITGBL1-depleted, or ITGBL1-overexpressed human articular chondrocytes. Increasing doses of 9EG7 antibody were applied to the ITGBL1-overexpressed cells to activate integrins. **n**: Control=20, siRNA=25, Itgbl1-OE=17, Itgbl1-OE+312 ng/ml=25, Itgbl1-OE+390 ng/ml=24, Itgbl1-OE+468 ng/ml=23. Scale bars: 20 μm. Data are shown as mean ± SEM (** $p<0.005$, *** $p<0.0005$).

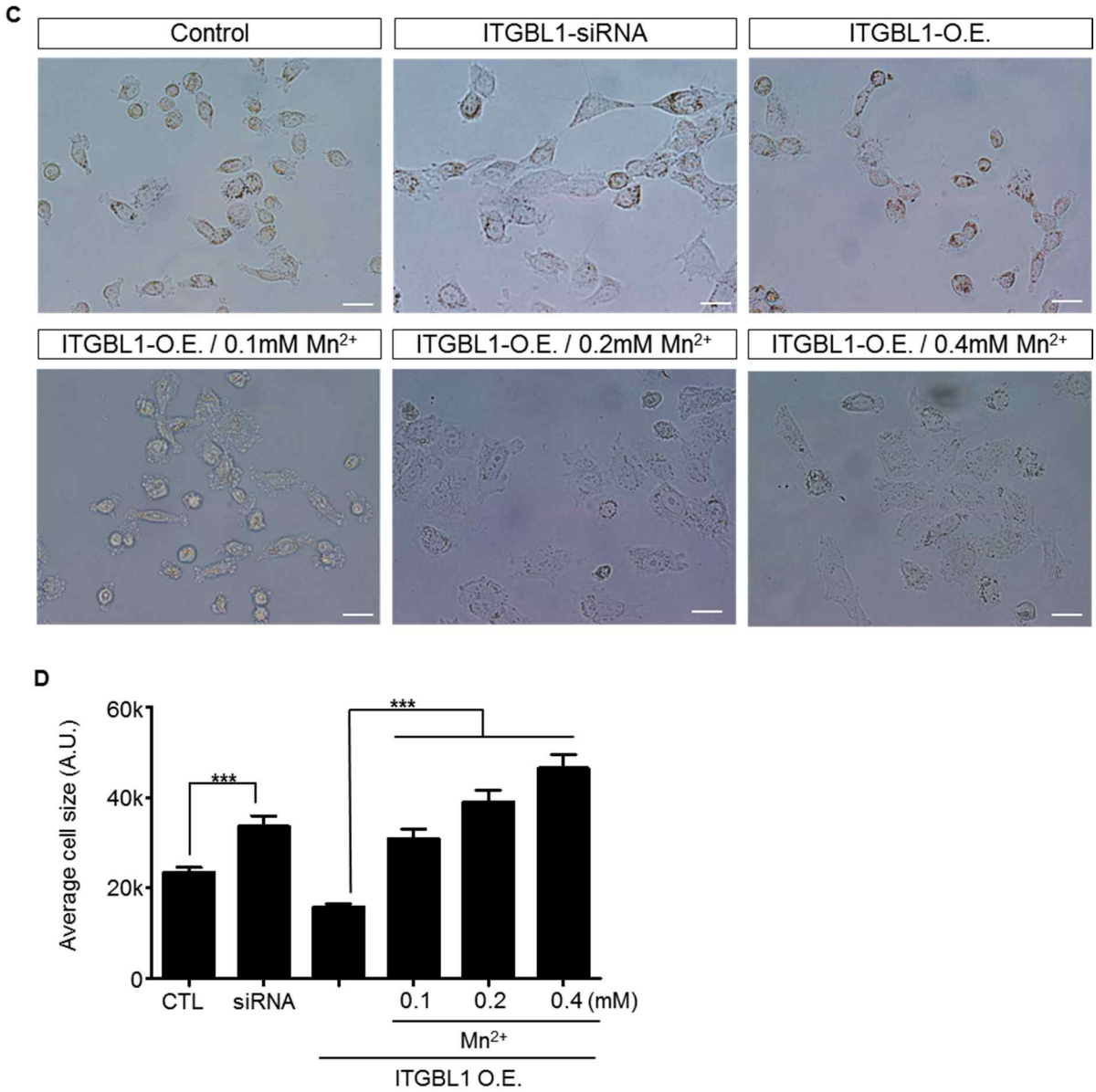

Figure 2-4-2. . ITGBL1 inhibits integrin-ECM complex formation in various cell types including chondrocytes.

C-D. Images of cell adhesion and spreading and quantification of cell size in control, ITGBL1-depleted, or ITGBL1-overexpressing PC3 cells. Increasing doses of Mn^{2+} were added to the ITGBL1-overexpressing cells to activate integrins. **n**: Control=54, siRNA=60, Itgbl1-OE=54, Itgbl1-OE+0.1 mM=45, Itgbl1-OE+0.2 mM=43, Itgbl1-OE+0.4 mM=37. Scale bars: 20 μm.

Integrin mediates cell-ECM binding through its extracellular domain and recruits proteins such as FAK and vinculin through its intracellular domain to form focal adhesion complexes and to transduce downstream signals. ITGBL1 depletion increased the number of FAK-positive focal adhesion complexes remained on collagen-coated plates, when we isolated focal adhesion complexes after removing cell bodies as previously described. Likewise, ITGBL1 depletion increased focal adhesion in PC3 cells as shown by integrin-β1 antibody staining (Fig. 2-3-2G, H). Using an active-form-specific integrin-β1 antibody and fluorescence-activated cell sorting (FACS), we saw that *Itgbl1* overexpression reduced the amount of active integrin-β1, whereas siRNA-mediated ITGBL1 depletion increased the amount of active integrin-β1 (Fig. 2-3-3I, J). In co-immunoprecipitation assays, ITGBL1 bound strongly to integrin-β1 in the presence, but not in the absence, of Ca^{2+} (Fig. 2-3-3K). Although we do not understand the physiological importance of this Ca^{2+}-dependent binding, the EGF domain has been shown to change its conformation upon calcium binding [82-84]. Furthermore, Notch signaling is regulated by the EGF domain in a Ca^{2+}-dependent manner [85, 86]. We further observed that *Itgbl1* overexpression reduced the phosphorylation of FAK and ERK 1/2 (Fig. 2-3-3L).

We next examined whether activation of integrin could overcome the ITGBL1-mediated loss of integrin-ECM binding. To that end, we treated the *Itgbl1*-overexpressed cells with integrin-activating antibody 9EG7 (Fig2-4-1A-B); however, the activating antibody did not efficiently recover cell spreading and attachment to the fibronectin-coated plates in the *Itgbl1*-overexpressed cells. We suspected that ITGBL1 may physically block the binding of the activating antibody to the integrin, or that structural changes in integrin induced by ITGBL1 may hinder the integrin-antibody interaction. Using Mn^{2+} [87] or DTT [88], which are pan integrin activators [89], we treated *Itgbl1*-overexpressing PC3 cells and performed a cell-spreading assay. As expected, activation of integrins by Mn^{2+} ions almost completely reversed integrin-ECM interactions in *Itgbl1*-overexpressing cells (Fig. 2-4-2C, D). PC3 cells are

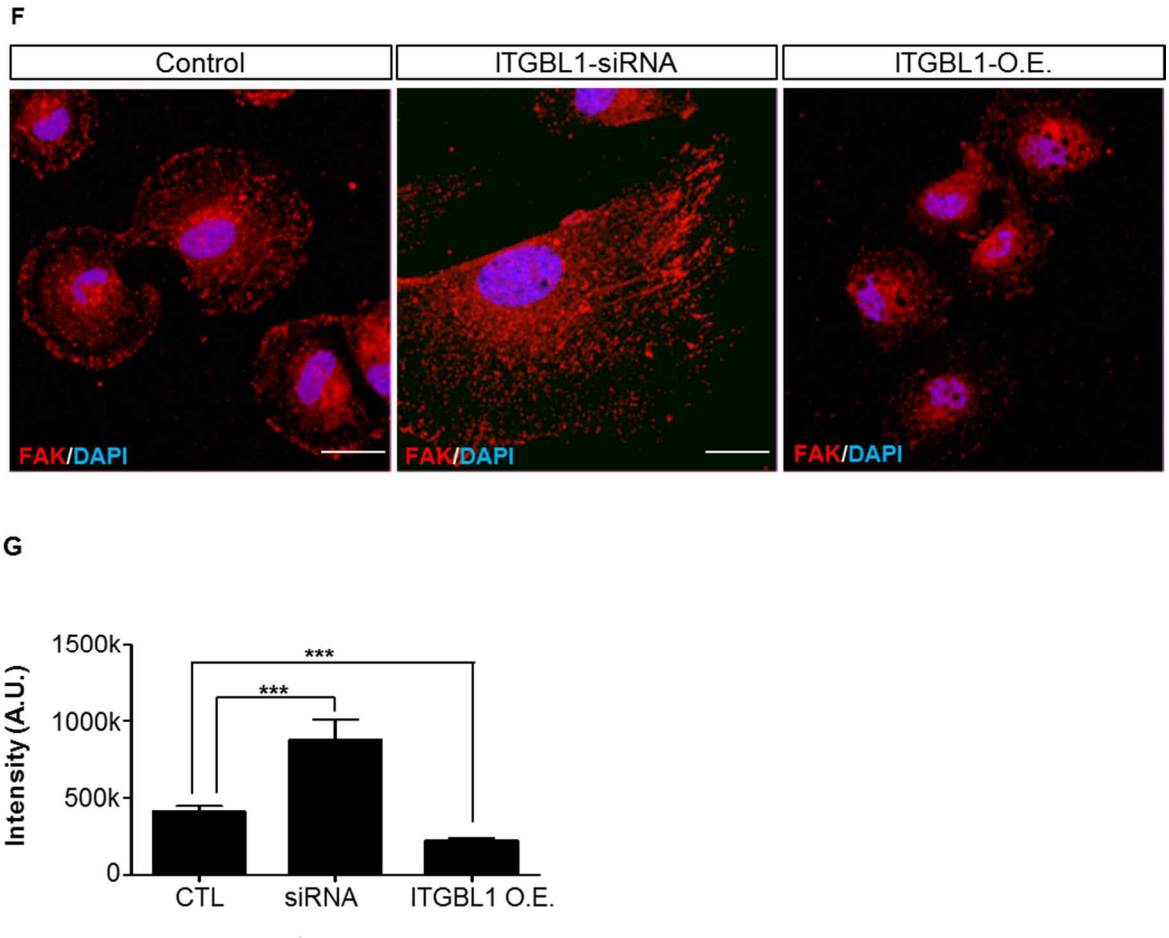

Figure 2-4-3. ITGBL1 inhibits integrin-ECM complex formation in various cell types including chondrocytes.

F-G. Immunofluorescent images using anti-FAK antibody (**C**) and the quantification of FAK intensity (**D**) in control, ITGBL1-depleted, or ITGBL1-overexpressing human chondrocytes. n:Control=13, siRNA=8, Itgbl1-OE=14. Scale bars: 10 μm.

prostate cancer cells and may intrinsically differ from chondrocytes. Therefore, we examined whether ITGBL1 also functions as an integrin inhibitor in human chondrocytes isolated from fetal femoral cartilages. Consistent with the PC3 cell data, ITGBL1 depletion significantly (p<0.0005) increased focal adhesion formation, whereas overexpression of *Itgbl1* reduced it

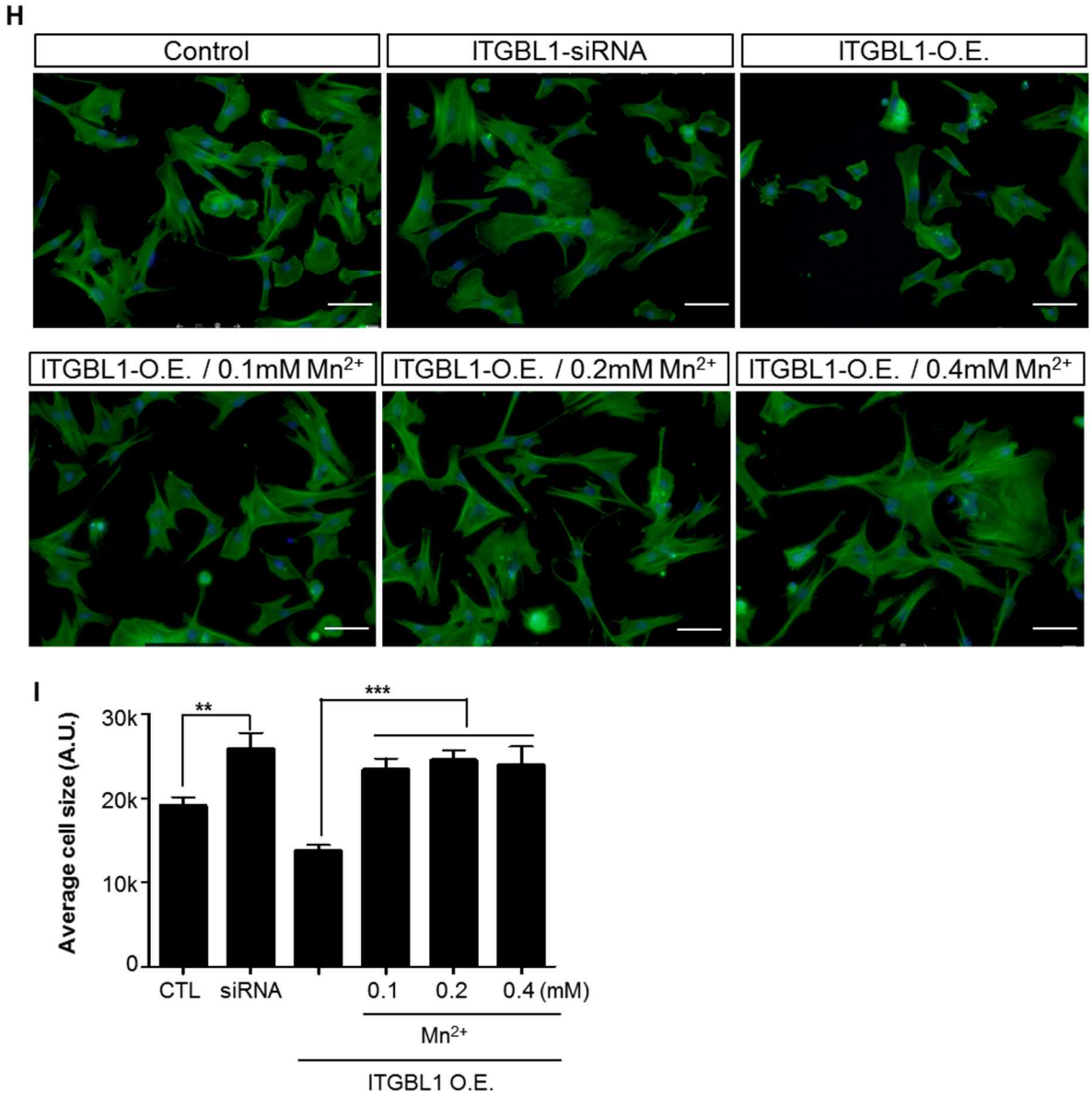

Figure 2-4-4. ITGBL1 inhibits integrin-ECM complex formation in various cell types including chondrocytes.

H-I. Images of cell adhesion and spreading and quantification of cell size in control, ITGBL1-depleted, or ITGBL1-overexpressing human articular chondrocytes. Increasing doses of Mn^{2+} were added to the ITGBL1-overexpressing cells to activate integrins. **n**: Control=70, siRNA=48, ITGBL1-OE=81, ITGBL1-OE+0.1 mM=53, ITGBL1-OE+0.2 mM=54, ITGBL1-OE+0.4 mM=31. Scale bars: 20 μm. Data are shown as mean ± SEM (** $p<0.005$, *** $p<0.0005$).

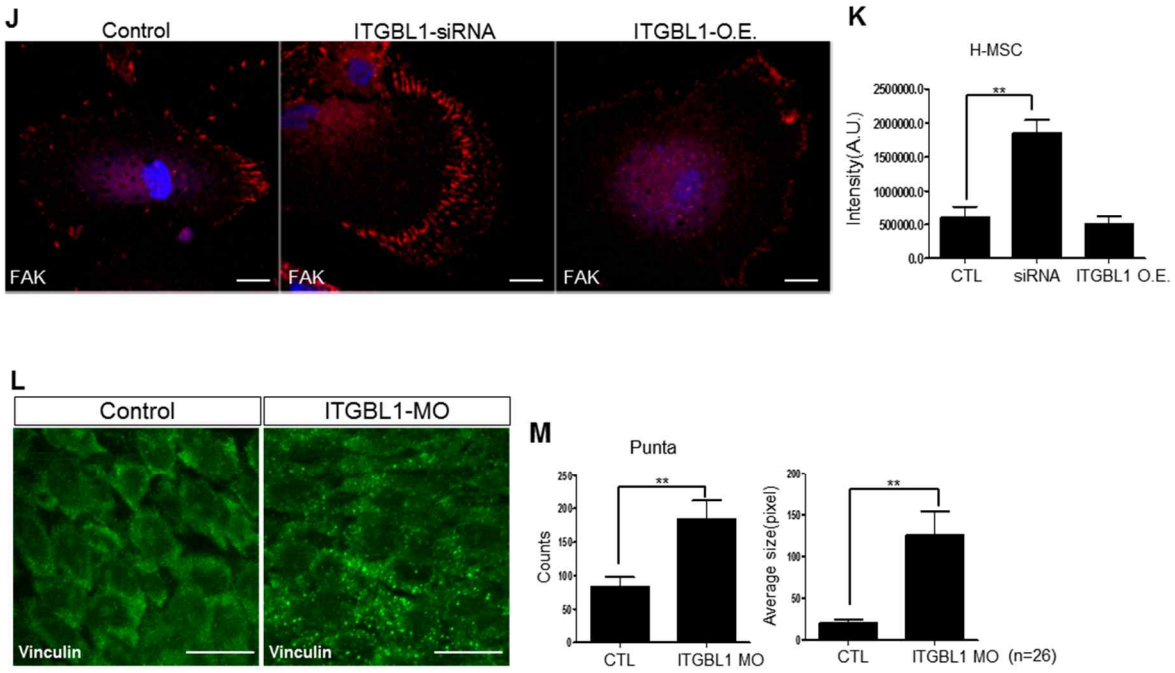

Figure 2-4-5. ITGBL1 inhibits focal adhesion-complex formation.

J-K. FAK-positive focal adhesion complexes were visualized in control, ITGBL1-depleted, or ITGBL1-overexpressed human BMSCs. **L-M.** ITGBL1 depletion increased vinculin-positive foci in prechondrocytes of *Xenopus* embryos at stage 37. Scale bars: 20 μm.

(Fig. 2-4-3F, G). Furthermore, this reduction of integrin-ECM interaction was fully recovered by activation of integrin by Mn^{2+} treatment (Fig. 2-4-4H, I). We also confirmed that ITGBL1 functions in a similar manner in hBMSCs and in prechondrocytes in *Xenopus* facial cartilage (Fig. 2-4-5J-M). Thus, our results suggest that ITGBL1 has a conserved role in inactivating integrin.

ITGBL1 promotes chondrogenesis via integrin inactivation.

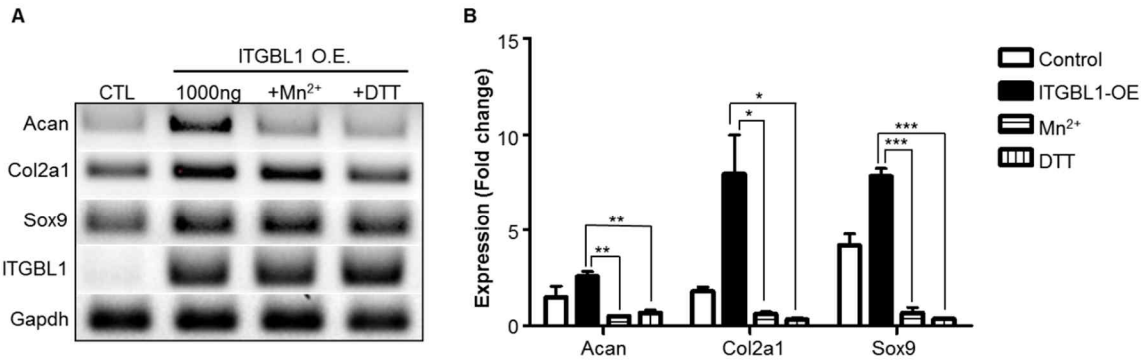

Figure 2-5-1. ITGBL1 promotes chondrogenesis via integrin inhibition.

A-B. Chondrogenic protein expression in ITGBL1-overexpressing ATDC5 cells treated with Mn^{2+} or DTT. **B.** Quantification of A; three replicate experiments).

Next, we investigated the possibility that integrin inactivation by ITGBL1 is a major mechanism promoting chondrogenesis. To this end, we exploited the ability of Mn^{2+} and DTT to activate integrin in *Itgbl1*-overexpressing ATDC5 cells. Upregulation of chondrogenic markers, such as *Sox9*, *Acan*, and *Col2al,* was reduced upon activation of integrins by Mn^{2+} and DTT in the *Itgbl1*-overexpressing ATDC5 cells (Fig. 2-5-1A, B). Consistent with the chondrogenic gene expression data, the glycosaminoglycan (GAG) level and the average size of cartilage micromasses were significantly (p<0.005) reduced by the activation of integrin in *Itgbl1*-overexpressing micromasses (Fig. 2-5-2C-E). It was previously reported that isolated chondrocytes dedifferentiate in adherent monolayer-culture, whereas less adhesive culture methods such as suspensions or culture in agarose gel promote re-differentiation of the dedifferentiated chondrocytes [90-92]. Integrin activation has also been suggested to mediate non-chondrogenic ECM deposition in dedifferentiated chondrocytes [93]. FAK activation

during chondrogenesis impairs proper cartilage formation, and integrin-mediated cell adhesion components are among the major enriched proteins in OA samples [94]. In contrast, chondrocytes express diverse integrin subunits, such as integrins α1, α3, α5, α10, αV, β1, β3, and β5 [42]. Given the ECM-rich environment and the expression of various integrins in chondrocytes, this contradictory circumstance in chondrogenic tissues suggests that ITGBL1

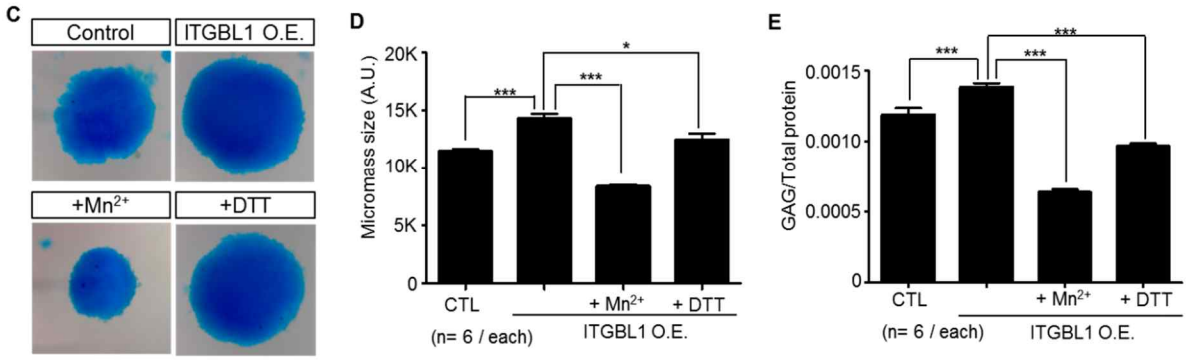

Figure 2-5-2. ITGBL1 promotes chondrogenesis via integrin inhibition.

C. Alcian blue staining in micromass cultures of control and ITGBL1-overexpressing ATDC5 cells in the presence of Mn^{2+} or DTT. Scale bars: 0.5mm **D-E.** The average size of micromasses and GAG/total protein ratio in C. n=6 for each experimental sample.

may possess a unique function as an integrin inhibitor during chondrogenesis. To determine which integrins are critical for the ITGBL1-mediated promotion of chondrogenesis, we first analyzed the expression of integrin subunits α1, α3, α5, α10, and β1, which are known to be expressed in monolayer-cultured chondrocytes [42]. Subunits α1, α5, and β1 were strongly expressed compared with subunits α3 and α10 in human chondrocytes (Fig. 2-5-3H). siRNA mediated knockdown of each integrin subunit in monolayer-cultured human chondrocytes confirmed that each siRNA effectively reduced the expression of the corresponding integrin subunit (fig. S10B). Integrin-β1 or integrin-α3 depletion most effectively increased Sox9 expression (Fig. 2-5-2F), although integrin-α5β1 was most strongly expressed (Fig. 2-5-3H).

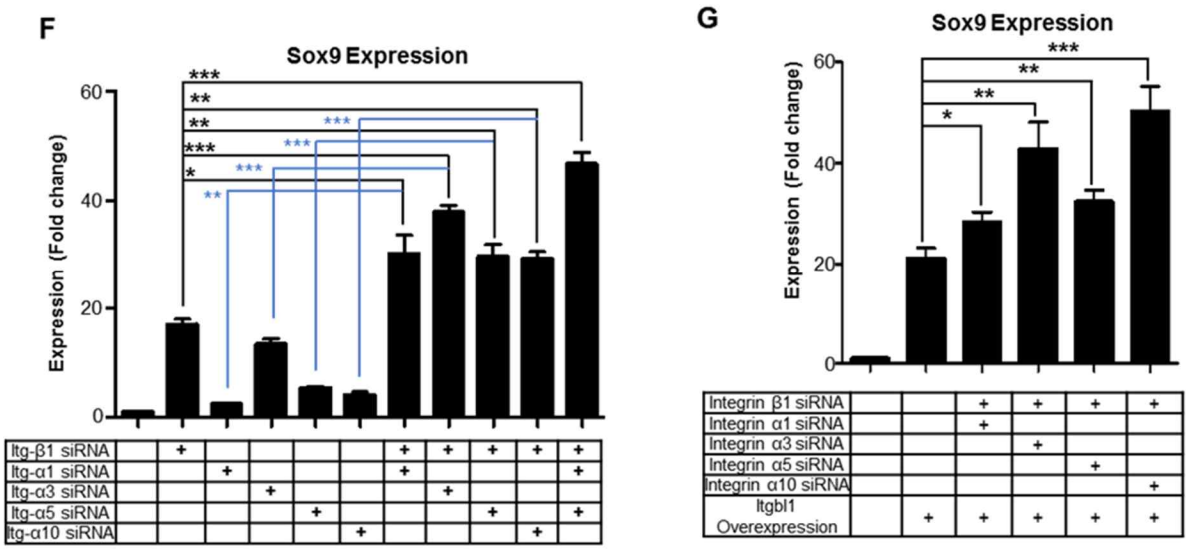

Figure 2-5-3. ITGBL1 promotes chondrogenesis via integrin inhibition.

F. Sox9 expression in human chondrocytes upon depletion of integrin-α1, 3, 5, or 10 in combination with β1 subunits analyzed by q-PCR. **G.** Sox9 expression in human chondrocytes upon depletion of integrin-α1β1, α3β1, α5β1, or α10β1 in combination with ITGBL1 overexpression analyzed by q-PCR. Data are shown as mean ± SEM from three replicate experiments (* $p<0.05$, ** $p<0.005$, *** $p<0.0005$)

However, co-depletion of each integrin-α subunit, which forms a heterodimer with integrin-β1, and β1 subunit synergistically induced *Sox9* expression at a similar extent (Fig. 2-5-3F). As expected, ectopic expression of *Itgbl1* increased *Sox9* expression synergistically with the depletion of every integrin subunit that we examined (Fig. 2-5-3G). Although our data are not able to conclusively verify the major integrin subunits interacting with ITGBL1, they strongly suggest that integrin signaling may exert negative effects on chondrogenesis and that ITGBL1 is an intrinsic factor promoting chondrogenesis via integrin inactivation. We suspect that ITGBL1 may inhibit a broad range of integrin subunits due to its synergy with various integrins.

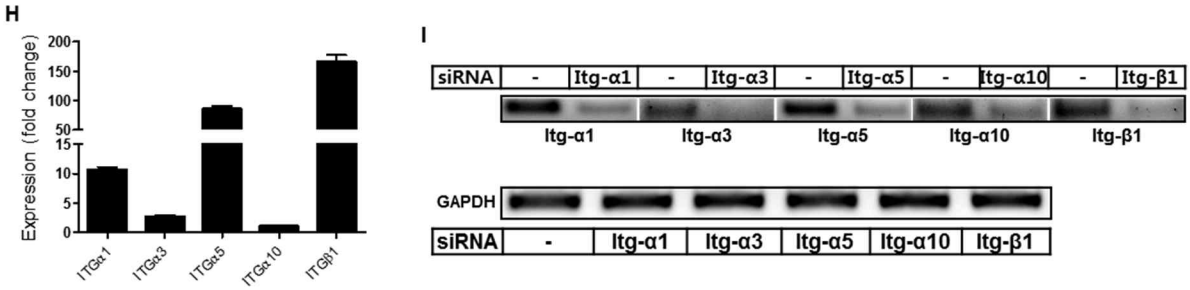

Figure 2-5-4. Relative expression of integrin subunits in human primary chondrocytes and efficacy of siRNA used in Figure 2-5-3F and 2-5-3G.

H. Integrins α1 and α5 are highly expressed along with integrin-β1 in human primary chondrocytes. **I.** siRNA transfection effectively decreased integrin expression.

ITGBL1 suppresses catabolic gene expression in chondrocytes.

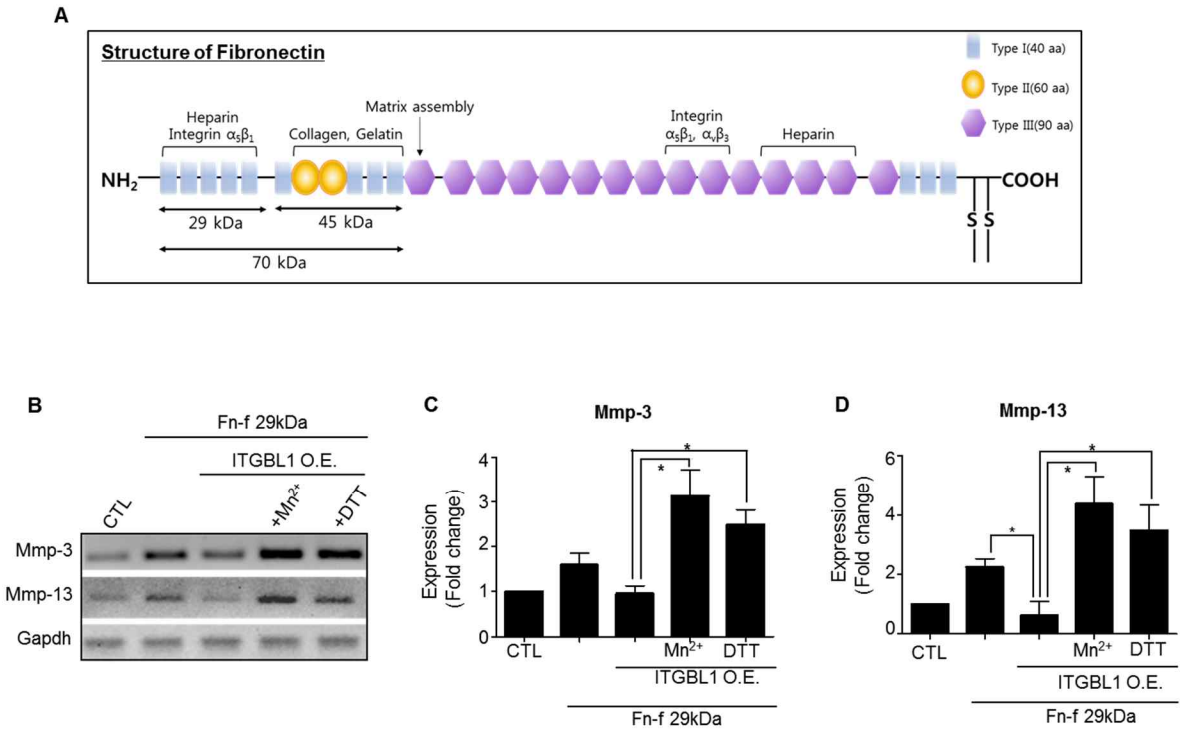

Figure 2-6-1. ITGBL1 protects chondrocytes form catabolic gene expression.

A. Structure of Fibronectin. B. Mmp3 and Mmp13 expression analyzed by RT-PCR after treatment of control or ITGBL1-overexpressing human chondrocytes with 29-kDa Fn-f. ITGBL1-overexpressing cells were treated with Mn^{2+} or DTT to activate integrins. **C-D**. Quantification of Mmp3 **C** or Mmp13 expression shown in **B**.

Integrin signaling not only modulates chondrogenesis but also is critically involved in destructive cartilage diseases. Fragmented ECM molecules, including fibronectin, activate inflammatory signals in various cells in articular cartilage tissue and promote the expression of catabolic factors, such as *Mmp13, Adamts5, Cox-2* (*Cyclooxygenase-2*), *IL-6* (*Interleukin-6*), and *IL-8* [66, 95]. Thus, we examined the potential protective function of ITGBL1 in arthritis development using human chondrocytes. Treatment of human chondrocytes with the N-terminal 29-kDa fragment of fibronectin (29-kDa Fn-fs) induced *Mmp3* and *Mmp13* expression

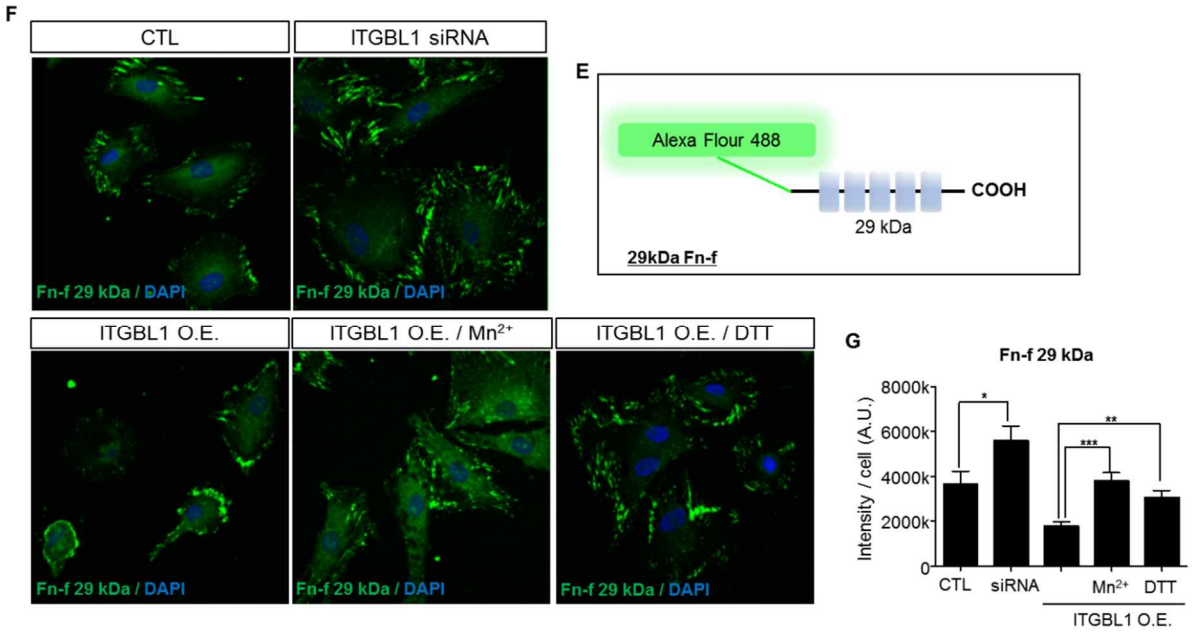

Figure 2-6-2. ITGBL1 protects chondrocytes form catabolic gene expression.

E. Alexa Fluor 488-conjugated 29-kDa Fn-fs. **F.** N-terminal 29-kDa Fn-f expression in control, ITGBL1-knockdown, and ITGBL1-overexpressing human chondrocytes. ITGBL1-overexpressing chondrocytes were treated with Mn^{2+} or DTT to activate integrins. **G**. Quantification of fluorescence intensity in **F**. **n**: Control=14, siRNA=16, ITGBL1-OE=17, ITGBL1-OE+Mn^{2+}=16, ITGBL1-

(Fig. 2-6-1B). In contrast, overexpression of *Itgbl1* reduced *Mmp3* and *Mmp13* expression, and these reductions were abolished by activation of integrins (Fig. 2-6-1B-D). The protective function of ITGBL1 against catabolic gene expression is likely due to integrin inactivation and subsequent reduction in fragmented ECM molecules binding to the chondrocytes. To directly examine this idea, we treated human chondrocytes with Alexa Fluor 488-conjugated 29-kDa Fn-fs (Fig. 2-6-2E). Depletion of ITGBL1 significantly (p<0.05) promoted binding of the 29-kDa Fn-fs compared to control cells (Fig. 2-6-2F, G), whereas overexpression of *Itgbl1* reduced binding (Fig. 2-6-2F, G). Furthermore, activation of integrin in *Itgbl1*-overexpressing chondrocytes restored the binding of Fn-fs to the cells (Fig. 2-6-2F, G).

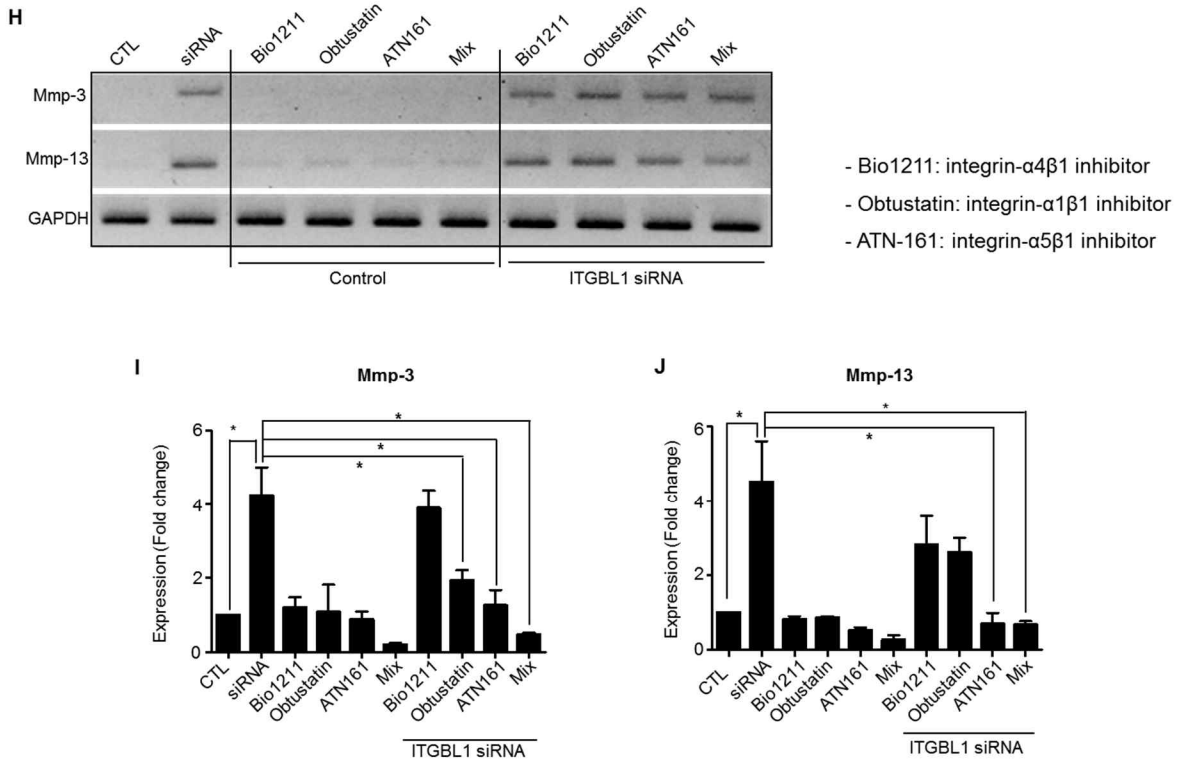

Figure 2-6-3. ITGBL1 protects chondrocytes form catabolic gene expression.

H. Mmp3 and Mmp13 expression analyzed by RT-PCR in control and ITGBL1-depleted human chondrocytes treated with various integrin inactivation. **I-J**. Quantification of (**H**). (* $p<0.05$, ** $p<0.005$, *** $p<0.0005$). Scale bars: 20 μm.

Next, we examined which integrin subtypes are mainly responsible for the catabolic gene expression using treatment with fragmented fibronectin and subtype-specific integrin inhibitors Bio1211 (integrin-α4β1 inhibitor), obtustatin (integrin-α1β1 inhibitor), and ATN-161 (integrin-α5β1 inhibitor). Although treating cells with all inhibitors together was most effective, among the inhibitors ATN-161 was more effective than the others in reducing *Mmp3* and *Mmp13* expression increased by ITGBL1 depletion (Fig. 2-6-3H-J). These data suggest that ITGBL1 has a dual function in chondrocytes, promoting chondrogenesis and protecting against catabolic gene expression, mediated through modulation of integrin activities.

ITGBL1 depletion results in OA-like cartilage damage in knee joints.

Next, we examined whether depletion of ITGBL1 causes cartilage damage in vitro and in a mouse model in vivo. We confirmed that ITGBL1 is expressed in chondrogenic limb mesenchyme and presumptive articular cartilage tissue and localizes to protrusions of ATDC5 cells, consistent with the *Xenopus* data (Fig. 2-1-1A-E). Although it localizes to the cell protrusions, ITGBL1 does not co-localize with the vinculin-positive stable focal adhesion complexes. In mouse chondrocytes, *Sox9* and *Col2a1* expression were reduced by adenoviral *Itgbl1*-shRNA (Ad-*Itgbl1* shRNA) infection and increased by ectopic *Itgbl1* expression using an adenoviral (Ad-*Itgbl1*) delivery system. Prior to the in vivo experiment, we tested the cytotoxicity and gene delivery of the adenoviral system. Ad-*Itgbl1*-infected cells showed no observable cytotoxicity based on MTT assay. Also, we confirmed by Ad-eGFP injection that the adenoviral system effectively delivered genes into mouse joint tissues. We speculated that depletion of ITGBL1 in mouse knee joint cartilage may result in OA-like phenotypes. Intra-articular injection of Ad-*Itgbl1* shRNA into wild-type mouse knee joints caused osteoarthritic cartilage destruction and reduced expression of COL2A1 and SOX9 in the joint cartilage. Furthermore, this OA-like cartilage destruction was partially recovered by inhibiting integrin activity by co-injecting integrin-α5β1 inhibitor ATN-161. We also observed that the catabolic genes MMP3/13 and ADAMTS5 were strongly induced in the ITGBL1-depleted cartilage whereas, in contrast, co-injection of ATN-161 reduced expression, consistent with the in vitro data shown in Fig. 2-5 and 2-6. However, we did not observe any change in osteophyte formation or subchondral bone thickness, although we observed a mild increase of synovial inflammation.

ITGBL1 protects cartilage tissue from OA development in the DMM mouse model.

We next examined if *Itgbl1* expression is affected by IL-1β treatment in mouse chondrocytes. IL-1β is an inflammatory factor involved in OA development and symptoms, and has been frequently used to examine OA pathogenesis [96]. Surprisingly, *Itgbl1* expression in mouse chondrocytes decreased upon IL-1β treatment, even before the reduction in *Col2a1* expression. Furthermore, overexpression of *Itgbl1* restored *Col2a1* and *Sox9* expression and reduced *Mmp3* and *Mmp13* expression in IL-1β-treated mouse chondrocytes (Fig. 2-6-1B-D), which is consistent with the human chondrocyte data (Fig. 6A-E). This result is surprising because IL-1β induces Mmp expression by signaling through the IL receptor and not through integrins. We hypothesize that the reduction of Mmp expression by ITGBL1 in IL-1β-treated mouse chondrocytes is due to synergistic interaction between IL-1β signaling and integrin signaling, as suggested in a recent study [97] which reported that IL-1β-responsive enhancer elements in *Mmp1* require ERK1/2 phosphorylation for *Mmp1* gene expression upon IL-1β treatment. Consistent with that hypothesis, *Itgbl1* overexpression strongly reduced ERK1/2 phosphorylation, and ITGBL1 depletion alone increased *Mmp3/13* expression (Fig.2-6-3H-J).

Upregulation of anabolic factors and downregulation of catabolic factors upon ectopic *Itgbl1* expression under pathological conditions suggested a possible protective role of ITGBL1 in OA development. We therefore collected joint cartilage tissue from human OA patients to analyze the expression of *Itgbl1*. *Itgbl1* expression was significantly (p=0.0001) reduced in cartilage from most OA patient. We next directly examined the role of ITGBL1 in OA pathogenesis using the surgical destabilization of the medial meniscus (DMM) mouse model of osteoarthritis. Intra-articular injection of Ad-*Itgbl1* into DMM-induced OA mice resulted in less severe OA-like cartilage damage and enhanced COL2A1 and SOX9 expression. We also observed reduced osteophyte formation, thickening of the subchondral bone plate, and

catabolic gene expression in Ad-*Itgbl1*-injected DMM-induced OA mice. Although DMM-induced OA was not strongly correlated with synovial inflammation, it was previously reported that DMM induces a low level of synovitis [98]. We observed a mild increase of synovial inflammation in Ad-*Itgbl1* infected joints; however, synovitis scores were not different between Ad-*Itgbl1*-infected samples regardless of DMM-operation, suggesting that ITGBL1 protects the cartilages directly rather than secondarily by modulating synovial inflammation. Taken together, our findings suggest that ITGBL1 not only promotes chondrogenesis in normal development but also exerts protective effects against cartilage damage.

2-4. Discussion

Here, we elucidated molecular functions of ITGBL1 in cartilage formation and OA development. ITGBL1 is transiently and specifically expressed in developing chondrocytes and promotes chondrogenesis. Our data suggest that ITGBL1 inhibits integrin signaling in developing chondrocytes. Developing chondrocytes constantly contact and interact with the surrounding ECM, and the major receptors for the ECM are integrins. Integrin-ECM interaction were shown to be necessary and to positively regulate prechondrocyte condensation [52-55], whereas other studies reported conflicting data about the functions of integrins in chondrogenic differentiation [31, 57, 58]. Integrin-ECM interactions promote osteogenic differentiation while inhibiting chondrogenesis in mesenchymal stem cells [31]. Increased FAK activation prevents chondrogenesis [81], and intrinsic FAK expression is actively downregulated in developing chondrocytes [99]. Furthermore, increased cell-ECM contacts is a key signal for dedifferentiation of chondrocytes [93, 100, 101]. These previous studies suggest that developing chondrocytes must dynamically regulate integrin activities for cartilage formation and for protection against dedifferentiation and OA. Given the complex ECM-rich environment and the expression of multiple integrin subunits, it is a challenge for chondrocytes to minimize integrin-ECM interactions to proceed through chondrogenic differentiation and also to maintain chondrogenic properties despite dedifferentiation signals. Our data suggest that developing chondrocytes accomplish this task by expressing ITGBL1 and actively inhibiting surface integrins that may otherwise mediate ECM-driven negative signaling.

Cell-ECM interaction is also critically involved in the pathology of destructive cartilage disorders. Cartilage damage induces expression of catabolic genes, such as Mmp and Adamts, which further damage cartilage and release fragmented ECM molecules into the synovial fluid.

These fragmented ECM molecules, such as fragmented fibronectin, are known to trigger catabolic gene expression in various cells in the articular tissues [62, 64]. Although there are conflicting reports regarding whether integrins are receptors for fragmented ECM molecules [62, 66-68], our data suggest that ITGBL1 reduces catabolic gene expression by inhibiting integrin activation. Further, we showed that ITGBL1 significantly reduces the binding of 29-kDa Fn-fs to chondrocytes. Fluorescence-labeled 29-kDa Fn-fs strongly localized to focal adhesions, which is interesting because that fragment binds fibrin or heparin but not the integrins [102]. Although a previous study showed differential distribution of Fn-fs to the cell surface [103], here we show that the Fn-fs binds to focal adhesion sites in human chondrocytes. Our data is most compatible with the hypothesis that integrin-mediated focal adhesions may recruit other unknown receptors for fibronectin fragments to the focal adhesomes, or integrins may have as yet unidentified binding sites for fragmented ECMs. Further in-depth study is needed to address these interesting questions.

We confirmed the protective role of ITGBL1 against OA development using an *in vivo* mouse model. The depletion of ITGBL1 induced OA-like damage in joint cartilages, which was partially recovered by the inhibition of integrin-α5β1 activity by ATN-161 peptide. Those results are consistent with a previous report that the chondrocyte-specific deletion of integrin-α5 protects against OA development [76]. Although ATN-161 co-injection did not fully recover the OA-like damage induced by ITGBL1 depletion, the lack of full recovery may have been due to the activation of other types of integrins that were not inhibited by ATN-161. We further confirmed the protective functions of ITGBL1 in a DMM-induced OA model. Compared with the severe loss and damage to the joint cartilages in DMM-operated mouse knee joints, ITGBL1 overexpression by viral transfection significantly reduced joint cartilage damage, suggesting ITGBL1 has therapeutic utility for improving OA symptoms. For the DMM model, we used 10-week-old male mice, as the sex and age are critical in OA

development. Although the age of mice at the time of DMM operation varies from 8 weeks to 12 weeks in the published literature, there is possibility that the skeletal system in 10-week-old mice is not fully mature and that the developmental program may affect the OA development. One study showed that DMM operation generally causes more severe OA in older mice than in younger mice [104], which suggests that the protective effects of ITGBL1 function may need to be examined further in older mice.

One limitation in the current study is the viral transfection system used, which does not specifically target chondrocytes in the joint tissues. Although 50% of chondrocytes were GFP positive, indicating transfection, synovial cells were also targeted by the viral transfection. Increasing recognition of the role of synovial inflammation in OA development has led to the concept that synovial inflammation is an active player in OA progression and increased pain [105]. Based on previous reports showing that fragmented ECM can affect various cell types in joint tissues, the ITGBL1 transfections may have not only reduced catabolic gene expression from chondrocytes but also reduced the production of proinflammatory factors from synovial cells or synovial fibroblasts. We believe that further tissue-specific induction of ITGBL1 will address this important issue. Fragmented ECM molecules not only target chondrocytes but also trigger inflammatory responses in other cells, such as synovial fibroblasts, macrophages, and immune cells, in inflammatory conditions such as rheumatoid arthritis [106]. This feed-forward cycling is mediated by the interaction between integrin and fragmented ECM molecules in a broad range of cell types in joint tissues. Several integrin inhibitors have been examined for the treatment of inflammatory arthritis [107-109]. Dozens of integrin subunits are dynamically expressed in various cell types involved in arthritis development. Given the subtype-specific nature of integrin inhibitors, it is very challenging to reduce integrin-mediated destructive signals from all cell types.

Increasing numbers of patients suffer from OA. However, most current treatments only relieve symptoms, and no approved medicines can effectively restore damaged cartilage. Here, we found that ITGBL1 expression in human chondrocytes from patients with OA is decreased. Our *in vivo* experiments showed that ITGBL1 not only has functions in cartilage development but also actively participates in maintaining cartilage and protecting it from destructive signals. Unlike other known integrin inhibitors, such as ICAP1, DOCK1, and SHARPIN1, ITGBL1 is secreted and reduces integrin signaling by physically interacting with integrin. The unique function of ITGBL1 as a secreted integrin inhibitor points toward new approaches to treat integrin-mediated human diseases and destructive cartilage disorders.

Chpater3. Concluding and Remarks

3.1 Summary and Conclusions

As started chapter1, this part describes the basic knowledge required for the understanding of experiments used in this doctoral dissertation. The experimental animals and signaling pathway for the study of the craniofacial development were briefly described.

In addition, chondrogenesis and integrin involved in cartilage formation important for facial formation were also described. And ITGBL is described briefly.

At chapter2, I described the function and role of ITGBL1 in the RNAseq of the pharyngeal arch of *Xenopus laevis*. ITGBL1 is β-integrin-related extracellular matrix protein which was first cloned and characterized from an osteoblast cDNA library. It contains ten EGF-like repeat domains and signal peptide for secretion. Functional studies using Morpholino confirmed that ITGBL is essential for cartilage formation. In addition, it has the same function in human cartilage formation process. Based on several papers that early integrin-ECM interaction may be required to promoted prechondrocyte condensation. And integrin-ECM interaction need to be inhibited for further decondensation, ECM secretion and cell shape change to complete chondrogenesis. In this process, ITGBL1 inhibits integrin-ECM interactions and this integrin inhibition enables chondrogenesis after prechondrocyte condensation. In this situation, I confirmed that ITGBL1 acts as an integrin inhibitor. As well as cartilage differentiation, the abnormal integrin signal can induce cartilage-related diseases. Fragmented ECM in OA patients binds to integrin of chondrocyte, synovial fibroblasts and immune cells. And, this binding increase catabolic factors and proinflammatory factor expression. Then this inflammation damages ECM again, and increases fragmented-ECM again. In this process,

ITGBL1 breaks the vicious circle of aggravating reaction and causing continuous cartilage, and promotes cartilage regeneration. Unlike known integrin inhibitory protein, ITGBL1 is secreted

And reduces integrin signaling by physically interacting with integrin. The unique function of ITGBL1 as a secreted integrin inhibitor points toward new approaches to treat integrin-mediated human diseases and destructive cartilage disorders. And it can be used as a biopharmaceutical and used as a cell therapy agent.

Supplements

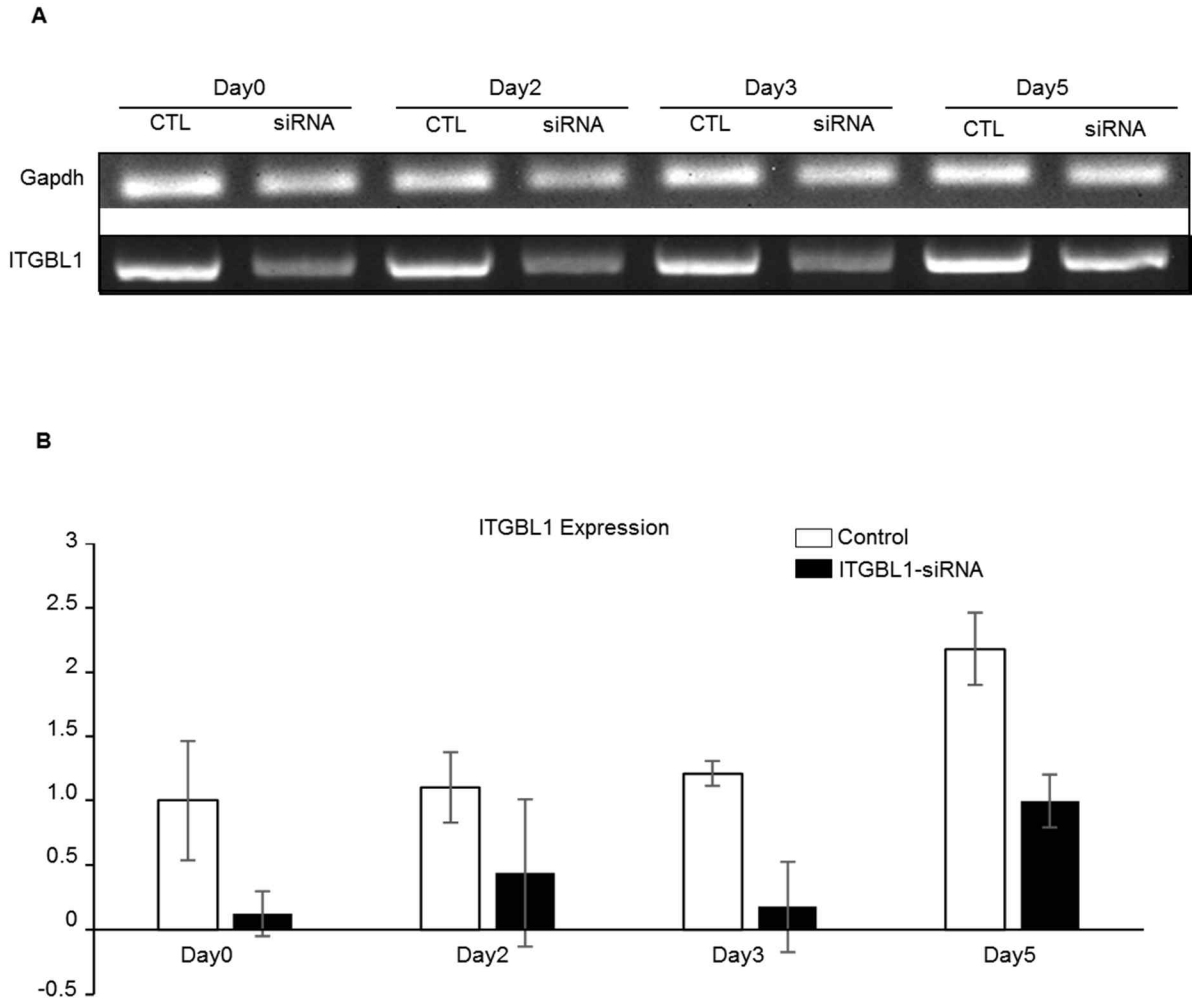

Figure S1. ITGBL1 expression during chondrogenesis analyzed after siRNA transfection.

A-B. ITGBL1 expression in human bone-marrow stem cells (hBMSCs) was analyzed by RT-PCR (**A**) and q-PCR (**B**) after siRNA transfection. Data are shown as mean ± SEM from three biological replicates.

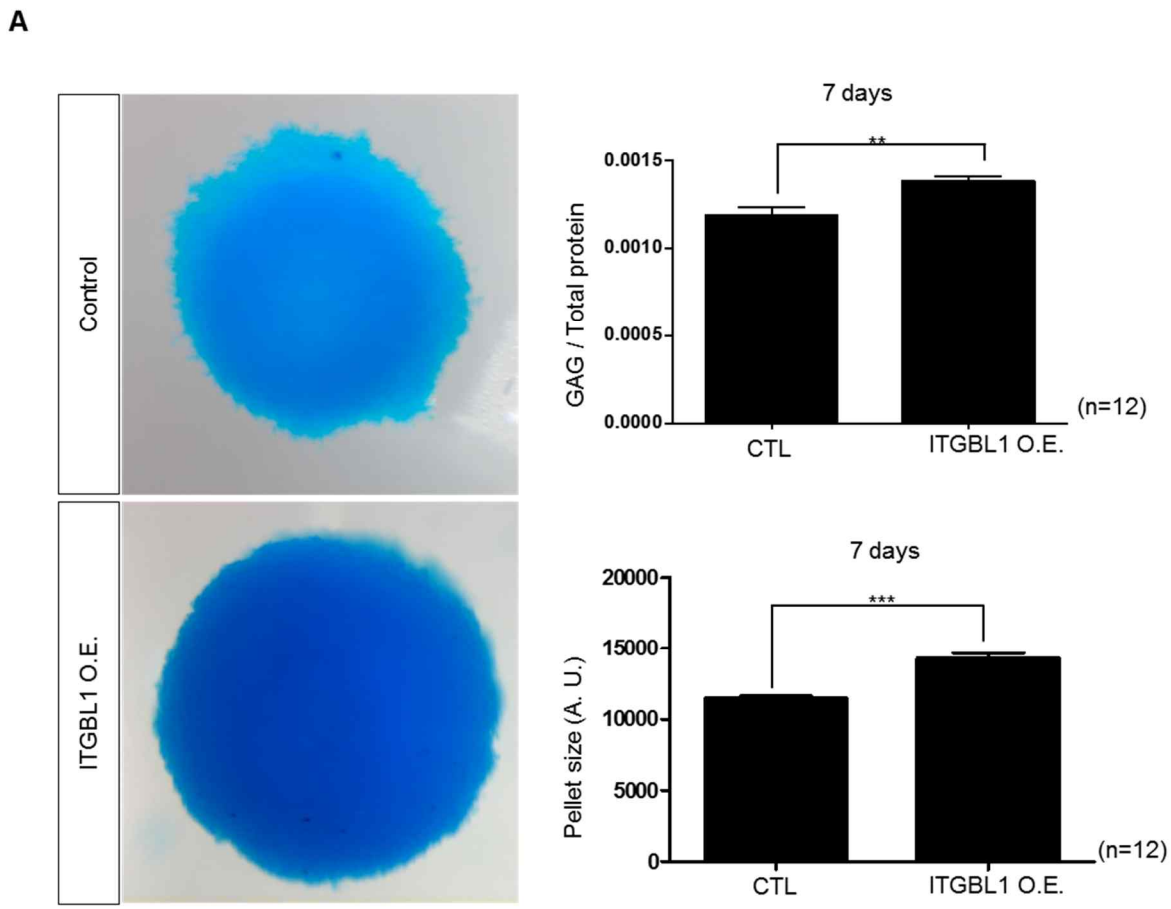

Figure S2. ITGBL promotes chondrogenesis.

A. Chondrogenic differentiation of micromass-cultured ATDC5 cells was analyzed by Alcian blue staining, and glycosaminoglycan (GAG) production was measured.

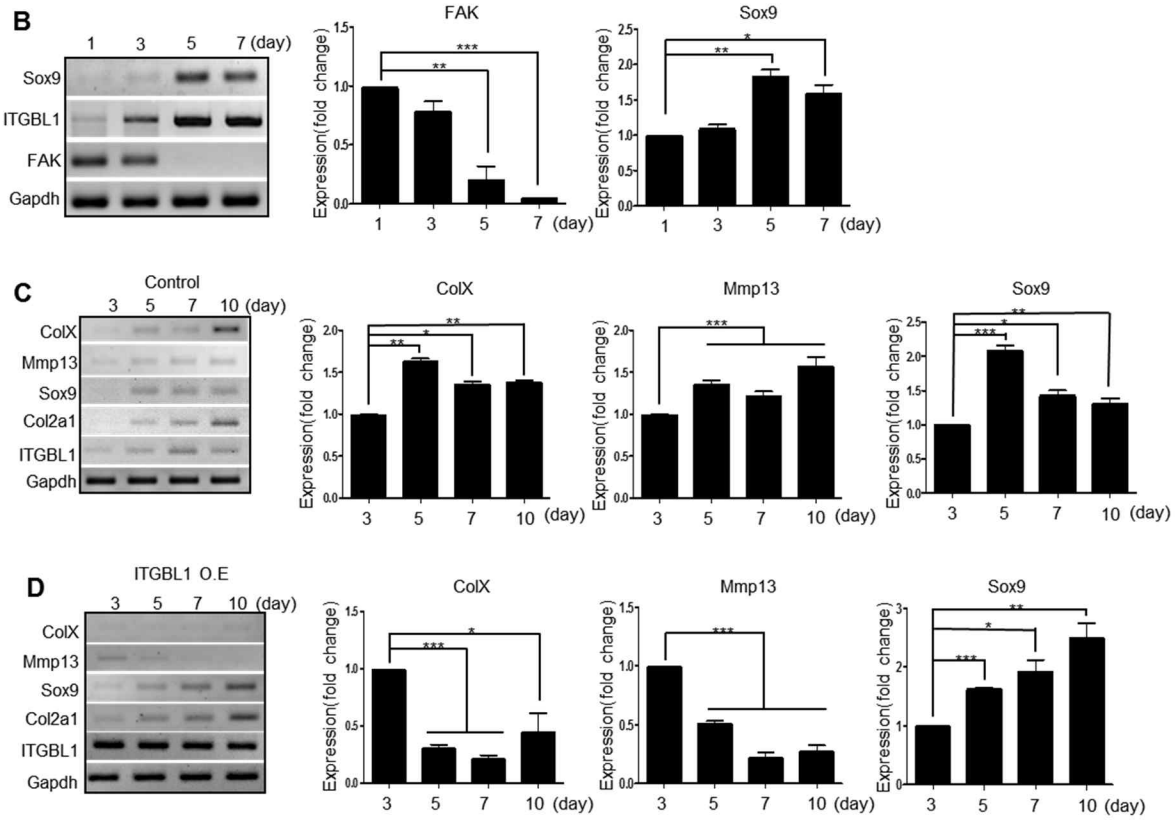

Figure S2-1. ITGBL promotes chondrogenesis.

B. FAK expression during chondrogenic differentiation of hBMSCs. The FAK level is almost completely repressed by Day 5 after chondrogenic induction. **C-D.** Hypertrophic maturation markers were analyzed during chondrogenic differentiation of ATDC5 cells in micromass culture after ITGBL1 overexpression (**G**). Data are shown as mean ± SEM from three replicate experiments

Supplementary Table S1. List of top 100 putative secreted proteins identified from transcriptome analysis.

List of top 100 putative secreted proteins that are differentially expressed in developing pharyngeal arches (Arch1, Arch2, and Arch3) and the dorsal/ventral parts of this region (ArchD and ArchV)

SeqID	log2FC	Arch1	Arch2	Arch3	ArchD	ArchV
LOC100491886.L|HS=TLL2|40|Xelaev18021897m	7.943	32.731	0.133	0.238	2.657	4.3
sst.S|HS=SST|100|Xelaev18029613m	7.869	43.723	0.611	0.187	1.929	8.099
clec19a.S|HS=CLEC19A|93|Xelaev18047527m	7.825	0.012	0.073	2.722	0.013	1.884
fstl3.L|HS=FSTL3|86|Xelaev18006463m	7.311	0.065	1.509	10.318	0.383	8.008
LOC100493098.L|HS=DNASE1L2|94|Xelaev18045463m	7.21	5.923	0.04	0.124	0.138	1.051
unnamed|HS=CA14|77|Xelaev18042787m	7.102	10.163	0.425	0.074	0.131	0.89
unnamed|HS=HGFAC|84|Xelaev18005068m	6.664	0.179	0.184	18.148	19.627	14.491
unnamed|HS=C4orf48|46|Xelaev18005037m	6.647	3.908	0.111	0.039	0.24	0.179
unnamed|HS=FETUB|74|Xelaev18029648m	6.635	0.115	1.254	11.427	46.345	10.328
unnamed|HS=FETUB|66|Xelaev18027506m	6.349	0.144	1.23	11.735	56.671	8.782
dct.L|HS=DCT|97|Xelaev18013152m	6.202	4.713	0.196	0.064	3.466	0.307
tyr.S|HS=TYR|100|Xelaev18016340m	6.135	2.178	0.048	0.031	1.507	0.117
unnamed|HS=TLL2|42|Xelaev18021894m	5.989	26.165	0.608	0.412	1.347	3.602
fgfbp3.L|HS=FGFBP3|86|Xelaev18034766m	5.668	6.202	0.122	0.593	0.229	0.735
c17orf67.L|HS=C17orf67|80|Xelaev18043803m	5.557	2.543	0.253	0.054	0.544	0.415
serpinc1.L|HS=SERPINC1|93|Xelaev18023232m	5.493	0.746	2.766	33.603	28.227	27.363

unnamed|HS=C4orf48|46|Xelaev18008874m	5.407	3.395	0.228	0.08	0.352	0.233
Xetrov90010415m.S|HS=NA|00|Xelaev18024389m	5.366	0.079	3.257	2.948	1.784	3.945
LOC101733976.S|HS=EDN3|55|Xelaev18046257m	5.293	6.859	0.175	0.198	1.025	1.698
unnamed|HS=CRISP3|77|Xelaev18028198m	5.239	2.115	0.056	0.19	0.222	0.451
unnamed|HS=AGR3|85|Xelaev18044817m	5.171	31.098	5.1	0.863	2.592	19.559
gbp6.1|HS=GBP1|70|Xelaev18001671m	5.037	0.095	0.636	3.119	0.55	2.308
LOC100490489.L|HS=NA|00|Xelaev18027216m	4.89	7.381	0.756	0.249	0.983	0.864
pcdh8.2.S|HS=PCDH8|70|Xelaev18015747m	4.856	0.334	2.276	9.672	3.254	6.536
npb.L|HS=NPB|84|Xelaev18043747m	4.783	3.552	0.285	0.129	0.153	0.208
slurp1l.L|HS=NA|00|Xelaev18023882m	4.659	5.888	0.233	0.287	0.34	1.482
LOC100485272-like.S|HS=ANGPT2|97|Xelaev18015134m	4.625	0.169	2.106	4.171	0.465	4.39
Xetrov90021952m.L|HS=TLL2|43|Xelaev18040194m	4.555	27.59	1.174	3.595	1.248	5.305
gdf7.L|HS=GDF6|85|Xelaev18028105m	4.507	0.239	1.846	5.436	6.902	0.795
pmel-like.S|HS=PMEL|58|Xelaev18015875m	4.109	22.369	4.832	1.296	7.076	4.256
tyrp1.L|HS=TYRP1|97|Xelaev18006806m	4.076	3.525	0.562	0.209	2.119	0.427
vwde.L|HS=VWDE|78|Xelaev18030909m	3.993	4.473	1.18	0.281	0.756	1.698
mcam-like.1|HS=MCAM|96|Xelaev18000065m	3.986	1.822	28.877	4.827	12.698	5.902
sfrp1.L|HS=SFRP1|88|Xelaev18018658m	3.951	3.629	14.22	56.137	21.051	53.337
apoc1-like.L|HS=NA|00|Xelaev18036025m	3.926	396.083	124.121	26.058	112.828	124.842
mxra5.L|HS=MXRA5|43|Xelaev18011748m	3.876	3.993	1.212	0.272	0.62	1.325
unnamed|HS=TLL1|44|Xelaev18021890m	3.871	80.83	17.585	5.526	18.007	37.359
fstl3.S|HS=FSTL3|87|Xelaev18009939m	3.871	0.41	1.178	6	0.503	5.87
hebp2.L|HS=HEBP2|79|Xelaev18026611m	3.862	7.083	0.976	0.487	0.71	1.197
apoe.L|HS=APOE|85|Xelaev18036024m	3.792	53.004	16.025	3.827	5.81	16.975
slc8a1-like.S|HS=SLC8A1|100|Xelaev18028910m	3.791	0.553	0.749	7.653	0.558	6.617

cpn1.S|HS=CPN1|87|Xelaev18037048m	3.728	20.386	2.279	1.539	6.064	4.589
LOC100496022.1|HS=PRSS27|92|Xelaev18001642m	3.708	21.708	7.858	1.661	3.825	13.988
c8b.L|HS=C8B|93|Xelaev18023028m	3.61	0.502	1.028	6.13	14.667	7.128
unnamed|HS=RBP4|89|Xelaev18037044m	3.608	17.786	15.571	1.459	9.927	4.092
itga7-like.L|HS=ITGA7|95|Xelaev18013342m	3.573	0.694	0.799	8.258	0.479	5.348
lrrn4.S|HS=LRRN4|97|Xelaev18028812m	3.506	0.337	0.967	3.828	1.595	5.497
LOC100487362.L|HS=LY9|32|Xelaev18040478m	3.505	2.838	1.656	0.25	0.178	0.367
rspo2.L|HS=RSPO2|100|Xelaev18032283m	3.424	6.911	2.565	0.644	1.476	1.476
pyy.S|HS=NPY|96|Xelaev18046061m	3.418	0.355	0.218	2.33	0.794	0.257
f2.S|HS=F2|98|Xelaev18024485m	3.414	0.39	0.933	4.157	4.675	3.267
sel1l3.S|HS=SEL1L3|95|Xelaev18008974m	3.29	2.298	0.685	0.235	0.336	1.208
unnamed|HS=LCN15|99|Xelaev18038205m	3.213	19.124	3.417	2.063	4.538	6.52
unnamed|HS=ANGPT1|101|Xelaev18032282m	3.155	0.28	0.597	2.494	1.191	1.104
nrn1.S|HS=NRN1|75|Xelaev18033414m	3.09	2.291	0.584	0.269	0.787	0.153
fibin.S|HS=FIBIN|100|Xelaev18024379m	3.049	1.484	12.282	3.127	6.681	3.054
olfml2a.S|HS=OLFML2A|96|Xelaev18041818m	3.046	7.192	1.606	0.871	1.836	2.419
tgfb2.S|HS=TGFB2|100|Xelaev18028671m	3.035	1.73	6.055	14.175	6.469	18.302
unnamed|HS=GP1BB|57|Xelaev18010547m	3.032	0.354	0.441	2.895	3.358	2.148
unnamed|HS=TECPR1|7|Xelaev18036521m	3	4.055	2.121	0.507	0.423	2.221
LOC100489571.S|HS=MMP8|97|Xelaev18016259m	2.96	1.139	8.863	4.084	0.027	3.147
ITGBL1.S|HS=ITGBL1|95|Xelaev18015636m	2.952	2.569	0.842	0.332	0.565	0.789
unnamed|HS=SCN4B|90|Xelaev18035439m	2.871	0.958	2.188	7.008	2.412	5.981
unnamed|HS=TMEM213|58|Xelaev18002504m	2.865	3.455	13.317	25.166	26.303	16.039
unnamed|HS=TNNT3|67|Xelaev18024361m	2.857	1.944	6.248	14.083	4.678	8.964
unnamed|HS=CRISP3|79|Xelaev18030177m	2.852	6.094	1.635	0.844	1.303	2.18
unnamed|HS=ANGPTL5|64|Xelaev18021227m	2.835	5.622	1.554	0.788	0.778	1.391
unnamed|HS=LOXL4|96|Xelaev18034711m	2.823	2.066	0.468	0.292	0.698	0.539

prrt3-like.L|HS=PRRT3|67|Xelaev18024053m	2.819	3.727	1.313	0.528	0.91	0.589
Xetrov90018420m.1|HS=ROBO4|99|Xelaev18003883m	2.79	2.325	3.695	16.082	8.331	10.299
Xetrov90024887m.L|HS=NA|00|Xelaev18043270m	2.786	6.387	1.799	0.926	0.743	2.384
fgf3.S|HS=FGF3|78|Xelaev18024490m	2.763	4.625	0.833	5.655	8.273	3.668
unnamed|HS=APELA|100|Xelaev18003936m	2.747	3.911	8.978	26.249	11.39	22.66
Xetrov90018420m.L|HS=ROBO1|17|Xelaev18035307m	2.712	2.853	3.26	18.696	13.616	8.351
nov.S|HS=NOV|88|Xelaev18033972m	2.691	0.99	3.13	6.393	6.832	2.166
unnamed|HS=NELL2|93|Xelaev18017595m	2.688	3.539	0.549	1.623	1.913	1.051
cdh15.S|HS=CDH15|96|Xelaev18024865m	2.654	6.662	15.01	2.384	5.413	7.229
igdcc3.L|HS=IGDCC3|89|Xelaev18018436m	2.64	4.418	2.005	0.709	2.334	1.009
fgf8.L|HS=FGF8|79|Xelaev18034665m	2.609	19.454	3.188	9.32	11.654	11.125
unnamed|HS=ATP6AP1|92|Xelaev18017668m	2.608	0.643	1.909	3.919	4.359	2.667
c6.2.L|HS=C6|100|Xelaev18008334m	2.588	0.925	1.463	5.56	6.348	4.378
unnamed|HS=CA4|90|Xelaev18010514m	2.569	2.391	0.566	0.403	0.673	0.462
clec19a.L|HS=CLEC19A|83|Xelaev18045207m	2.558	0.525	1.552	3.091	0.9	2.85
unnamed|HS=CACNA2D4|93|Xelaev18003010m	2.556	1.986	1.461	8.592	6.055	3.817
unnamed|HS=NELL2|93|Xelaev18021119m	2.541	2.218	0.381	0.39	1.124	0.573
unnamed|HS=KDR|96|Xelaev18009068m	2.525	1.047	5.879	6.025	3.959	7.705
fam132a.S|HS=FAM132A|107|Xelaev18037500m	2.514	0.426	0.895	2.433	0.411	2.035
LOC101733976.L|HS=EDN3|53|Xelaev18043542m	2.449	2.544	1.992	0.466	2.728	1.195
nog2.S|HS=NOG|95|Xelaev18047671m	2.448	2.93	1.76	0.537	0.86	0.411
npr3-like.L|HS=NPR3|90|Xelaev18008385m	2.429	8.499	3.773	1.578	2.862	2.916
unnamed|HS=LY86|82|Xelaev18031614m	2.396	2.379	0.482	0.452	0.929	0.547
Xetrov90000623m.L|HS=SHISA3|93|Xelaev18005242m	2.381	7.436	6.743	1.428	1.119	4.449
ramp2.L|HS=RAMP2|61|Xelaev18043825m	2.377	1.44	3.696	7.482	5.008	3.22
igfbpl1.L|HS=IGFBPL1|74|Xelaev18006653m	2.372	4.945	8.355	1.614	6.356	4.638

stc2.L|HS=STC2|104|Xelaev18017248m	2.37	42.763	18.002	8.272	11.249	12.744
LOC100496170-like.1|HS=IZUMO1R|68|Xelaev18000799m	2.37	11.898	2.97	2.301	3.944	4.662
prtn3-like.1.L|HS=PRTN3|85|Xelaev18006264m	2.367	0.524	1.797	2.704	0.556	1.014
fgfbp2.L|HS=FGFBP2|99|Xelaev18005148m	2.359	15.019	14.741	2.928	0.936	12.958
unnamed|HS=CFI|105|Xelaev18005652m	2.32	3.237	7.08	16.167	28.023	12.637
mmp11.S|HS=MMP11|92|Xelaev18010511m	2.316	3.304	2.639	13.137	1.768	11.177

Acknowledgements

지난 7 년동안 느리고 많이 부족하지만 믿어주시고 기다려주신 교수님께 감사합니다. 박사 과정 동안 많은 것을 배웠고 제가 살아가면서 좋은 경험과 밑거름이 될 것이라 생각합니다.

바쁘신 일정에도 박사 학위 심사에 참여 해주신 권태준 교수님, 박찬영 교수님, 김정범 교수님 그리고 경북대 이현식 교수님 이 자리를 빌어 감사의 말씀 전하고 싶습니다. 저에게 주신 따끔한 충고 흘려 버리지 않고 살이 될 수 있도록 더 노력하고 배우겠습니다. 그리고 유니스트에서 정말 많은 동료들을 알게 되었습니다. 저에게 언니 같이 선생님 같이 충고해 주시고 관심을 가져주신 혜경언니, 지은언니, 그리고 우리 막내 현아 정말 감사하고 이분들 덕분에 학교생활이 즐거웠고 뜻 깊었습니다.

7 년 동안 함께 했던 효정아 실험실의 궂은 일과 업무를 투정하지 않고 다른 멤버들에게 피해가 가지 않도록 잘 해 주고 배려해 줘서 정말 고맙다. 그리고 언니가 하는 모든 부탁 언제나 웃으며 도와 주고, 힘들 때 함께해 줘서 박사 과정이 힘들지 않았어. 넌 어디서든 가서 사랑 받을 거야.

그리고 7 년 동안 함께 했던 동길아 언제나 누나들 배려해 주고 생각해주는 마음 정말 고마웠어. 알아 가면서 더더욱 유쾌하고 누나들 즐겁게 해줬던 동길이 덕분에 실험실이 즐거웠고 웃음이 떠나가질 않았던 것 같아.

항상 아픈 손가락 근영아. 누나 눈치 보면서 생활하느라 고생했다. 누나가 쓴 소리 해도 웃어 넘기며 배려해주는 마음 말 안 해도 누나는 알고 있어. 이제 박사과정이니깐 너가 맡은 일에 좀더 적극적이고 최선을 다했으면 좋겠다. 그리고 하은아 막내로서 많은 일은 하면서 언니, 오빠들 눈치 보느라 고생이 많다. 항상 먼저 다가와 언니가 뭐가 필요한지 물어봐 주고 언니 바

쁠 때 눈치껏 알아서 척척해가는 하은이 힘들겠지만 열심히 하는 너의 모습 정말 보기가 좋아.

모든 저의 랩 멤버들 힘들 때 마다 서로 격려해주고 제가 마지막 논문을 내기까지 많이 참아 주고 자기 일처럼 걱정해주고 양보해 주었습니다. 정말 최고의 랩 멤버였다고 다시 한번 할 하고 싶습니다.

제가 늦은 나이에 과정을 시작하여 많이 걱정하시고 아낌없이 지원해주신 저의 부모님께 정말 감사하며, 그리고 항상 걱정하는 마음과 같은 일은 하면서 묵묵히 지켜 봐주고 의지할 수 있게 든든한 동반자로서의 역할을 해준 저의 남편에게도 고맙다는 말을 하고 싶습니다.

모두 언급을 하지 못했지만 저를 도와 주신 모든 분들께 이 기회를 통해 감사의 말씀을 드립니다. 마지막으로 이 논문을 마무리 할 수 있게 도와 주신 저의 교수님께 다시 한번 감사 드립니다.

References

1. Akkiraju, H. and A. Nohe, *Role of Chondrocytes in Cartilage Formation, Progression of Osteoarthritis and Cartilage Regeneration.* J Dev Biol, 2015. **3**(4): p. 177-192.
2. Solchaga, L.A., K.J. Penick, and J.F. Welter, *Chondrogenic differentiation of bone marrow-derived mesenchymal stem cells: tips and tricks.* Methods Mol Biol, 2011. **698**: p. 253-78.
3. Buckwalter, J.A., *Articular cartilage: injuries and potential for healing.* J Orthop Sports Phys Ther, 1998. **28**(4): p. 192-202.
4. Buckwalter, J.A. and H.J. Mankin, *Articular cartilage: degeneration and osteoarthritis, repair, regeneration, and transplantation.* Instr Course Lect, 1998. **47**: p. 487-504.
5. Mankin, H.J., *The reaction of articular cartilage to injury and osteoarthritis (first of two parts).* N Engl J Med, 1974. **291**(24): p. 1285-92.
6. Mankin, H.J. and J.A. Buckwalter, *Restoration of the osteoarthrotic joint.* J Bone Joint Surg Am, 1996. **78**(1): p. 1-2.
7. Danilchick, M., H.B. Peng, and B.K. Kay, *Xenopus laevis: Practical uses in cell and molecular biology. Pictorial collage of embryonic stages.* Methods Cell Biol, 1991. **36**: p. 679-81.
8. Keller, E.F., *Drosophila embryos as transitional objects: the work of Donald Poulson and Christiane Nusslein-Volhard.* Hist Stud Phys Biol Sci, 1996. **26**(2): p. 313-46.
9. Dean, S., et al., *A surface transporter family conveys the trypanosome differentiation signal.* Nature, 2009. **459**(7244): p. 213-7.
10. Dascal, N., *The use of Xenopus oocytes for the study of ion channels.* CRC Crit Rev Biochem, 1987. **22**(4): p. 317-87.
11. Vincent, J.P. and J.C. Gerhart, *Subcortical rotation in Xenopus eggs: an early step in embryonic axis specification.* Dev Biol, 1987. **123**(2): p. 526-39.
12. Johnston, M.C., *A radioautographic study of the migration and fate of cranial neural crest cells in the chick embryo.* Anat Rec, 1966. **156**(2): p. 143-55.
13. Le Lievre, C.S., *Participation of neural crest-derived cells in the genesis of the skull in birds.* J Embryol Exp Morphol, 1978. **47**: p. 17-37.
14. Le Lievre, C.S. and N.M. Le Douarin, *Mesenchymal derivatives of the neural crest: analysis of chimaeric quail and chick embryos.* J Embryol Exp Morphol, 1975. **34**(1): p. 125-54.
15. Sadaghiani, B. and C.H. Thiebaud, *Neural crest development in the Xenopus laevis embryo, studied by interspecific transplantation and scanning electron microscopy.* Dev Biol, 1987. **124**(1): p. 91-110.
16. Creuzet, S., G. Couly, and N.M. Le Douarin, *Patterning the neural crest derivatives during development of the vertebrate head: insights from avian studies.* J Anat, 2005. **207**(5): p. 447-59.
17. Morales, A.V., J.A. Barbas, and M.A. Nieto, *How to become neural crest: from segregation to delamination.* Semin Cell Dev Biol, 2005. **16**(6): p. 655-62.
18. Steventon, B., C. Carmona-Fontaine, and R. Mayor, *Genetic network during neural crest induction: from cell specification to cell survival.* Semin Cell Dev Biol, 2005. **16**(6): p. 647-54.
19. Gammill, L.S. and M. Bronner-Fraser, *Neural crest specification: migrating into genomics.* Nat Rev Neurosci, 2003. **4**(10): p. 795-805.

20. Kulesa, P.M. and S.E. Fraser, *In ovo time-lapse analysis of chick hindbrain neural crest cell migration shows cell interactions during migration to the branchial arches.* Development, 2000. **127**(6): p. 1161-72.
21. Meulemans, D. and M. Bronner-Fraser, *Amphioxus and lamprey AP-2 genes: implications for neural crest evolution and migration patterns.* Development, 2002. **129**(21): p. 4953-62.
22. Kuratani, S., *Developmental studies of the lamprey and hierarchical evolutionary steps towards the acquisition of the jaw.* J Anat, 2005. **207**(5): p. 489-99.
23. Grenier, J., et al., *Relationship between neural crest cells and cranial mesoderm during head muscle development.* PLoS One, 2009. **4**(2): p. e4381.
24. Noden, D.M., *Patterns and organization of craniofacial skeletogenic and myogenic mesenchyme: a perspective.* Prog Clin Biol Res, 1982. **101**: p. 167-203.
25. Schilling, T.F. and C.B. Kimmel, *Segment and cell type lineage restrictions during pharyngeal arch development in the zebrafish embryo.* Development, 1994. **120**(3): p. 483-94.
26. Song, E.K. and T.J. Park, *Integrin signaling in cartilage development.* Animal Cells and Systems, 2014. **18**(6): p. 365-371.
27. Danisovic, L., I. Varga, and S. Polak, *Growth factors and chondrogenic differentiation of mesenchymal stem cells.* Tissue Cell, 2012. **44**(2): p. 69-73.
28. Arita, N.A., D. Pelaez, and H.S. Cheung, *Activation of the extracellular signal-regulated kinases 1 and 2 (ERK1/2) is needed for the TGFbeta-induced chondrogenic and osteogenic differentiation of mesenchymal stem cells.* Biochem Biophys Res Commun, 2011. **405**(4): p. 564-9.
29. Tian, H., et al., *Chondrogenic differentiation of mouse bone marrow mesenchymal stem cells induced by cartilage-derived morphogenetic protein-2 in vitro.* J Huazhong Univ Sci Technolog Med Sci, 2007. **27**(4): p. 429-32.
30. Lim, Y.B., et al., *Disruption of actin cytoskeleton induces chondrogenesis of mesenchymal cells by activating protein kinase C-alpha signaling.* Biochem Biophys Res Commun, 2000. **273**(2): p. 609-13.
31. Tang, Y., et al., *MT1-MMP-dependent control of skeletal stem cell commitment via a beta1-integrin/YAP/TAZ signaling axis.* Dev Cell, 2013. **25**(4): p. 402-16.
32. Giancotti, F.G. and E. Ruoslahti, *Integrin signaling.* Science, 1999. **285**(5430): p. 1028-32.
33. Humphries, M.J., *Integrin structure.* Biochem Soc Trans, 2000. **28**(4): p. 311-39.
34. Goldmann, W.H., et al., *Native talin is a dumbbell-shaped homodimer when it interacts with actin.* J Struct Biol, 1994. **112**(1): p. 3-10.
35. Calderwood, D.A., et al., *The Talin head domain binds to integrin beta subunit cytoplasmic tails and regulates integrin activation.* J Biol Chem, 1999. **274**(40): p. 28071-4.
36. Docheva, D., et al., *Integrin signaling in skeletal development and function.* Birth Defects Res C Embryo Today, 2014. **102**(1): p. 13-36.
37. Shattil, S.J., C. Kim, and M.H. Ginsberg, *The final steps of integrin activation: the end game.* Nat Rev Mol Cell Biol, 2010. **11**(4): p. 288-300.
38. Hynes, R.O., *Integrins: bidirectional, allosteric signaling machines.* Cell, 2002. **110**(6): p. 673-87.
39. Kim, S.H., J. Turnbull, and S. Guimond, *Extracellular matrix and cell signalling: the dynamic cooperation of integrin, proteoglycan and growth factor receptor.* J Endocrinol, 2011. **209**(2): p. 139-51.

40. Berg, R.W., et al., *Cloning and characterization of a novel beta integrin-related cDNA coding for the protein TIED ("ten beta integrin EGF-like repeat domains") that maps to chromosome band 13q33: A divergent stand-alone integrin stalk structure.* Genomics, 1999. **56**(2): p. 169-78.
41. Pitsillides, A.A. and F. Beier, *Cartilage biology in osteoarthritis--lessons from developmental biology.* Nat Rev Rheumatol, 2011. **7**(11): p. 654-63.
42. Loeser, R.F., *Integrins and chondrocyte-matrix interactions in articular cartilage.* Matrix Biol, 2014. **39**: p. 11-6.
43. LaPointe, V.L., A. Verpoorte, and M.M. Stevens, *The changing integrin expression and a role for integrin beta8 in the chondrogenic differentiation of mesenchymal stem cells.* PLoS One, 2013. **8**(11): p. e82035.
44. Varas, L., et al., *Alpha10 integrin expression is up-regulated on fibroblast growth factor-2-treated mesenchymal stem cells with improved chondrogenic differentiation potential.* Stem Cells Dev, 2007. **16**(6): p. 965-78.
45. Lapadula, G., et al., *Integrin expression on chondrocytes: correlations with the degree of cartilage damage in human osteoarthritis.* Clin Exp Rheumatol, 1997. **15**(3): p. 247-54.
46. Loeser, R.F., C.S. Carlson, and M.P. McGee, *Expression of beta 1 integrins by cultured articular chondrocytes and in osteoarthritic cartilage.* Exp Cell Res, 1995. **217**(2): p. 248-57.
47. Ostergaard, K., et al., *Expression of alpha and beta subunits of the integrin superfamily in articular cartilage from macroscopically normal and osteoarthritic human femoral heads.* Ann Rheum Dis, 1998. **57**(5): p. 303-8.
48. Almonte-Becerril, M., M. Costell, and J.B. Kouri, *Changes in the integrins expression are related with the osteoarthritis severity in an experimental animal model in rats.* J Orthop Res, 2014. **32**(9): p. 1161-6.
49. Newman, S.A., et al., *Multiscale models for vertebrate limb development.* Curr Top Dev Biol, 2008. **81**: p. 311-40.
50. White, D.G., et al., *Functional analysis of fibronectin isoforms in chondrogenesis: Full-length recombinant mesenchymal fibronectin reduces spreading and promotes condensation and chondrogenesis of limb mesenchymal cells.* Differentiation, 2003. **71**(4-5): p. 251-61.
51. Downie, S.A. and S.A. Newman, *Different roles for fibronectin in the generation of fore and hind limb precartilage condensations.* Dev Biol, 1995. **172**(2): p. 519-30.
52. Hirsch, M.S. and K.K. Svoboda, *Beta 1 integrin antibodies inhibit chondrocyte terminal differentiation in whole sterna.* Ann N Y Acad Sci, 1996. **785**: p. 267-70.
53. Aszodi, A., et al., *Beta1 integrins regulate chondrocyte rotation, G1 progression, and cytokinesis.* Genes Dev, 2003. **17**(19): p. 2465-79.
54. Terpstra, L., et al., *Reduced chondrocyte proliferation and chondrodysplasia in mice lacking the integrin-linked kinase in chondrocytes.* J Cell Biol, 2003. **162**(1): p. 139-48.
55. Garciadiego-Cazares, D., et al., *Coordination of chondrocyte differentiation and joint formation by alpha5beta1 integrin in the developing appendicular skeleton.* Development, 2004. **131**(19): p. 4735-42.
56. Chang, J.C., S.H. Hsu, and D.C. Chen, *The promotion of chondrogenesis in adipose-derived adult stem cells by an RGD-chimeric protein in 3D alginate culture.* Biomaterials, 2009. **30**(31): p. 6265-75.
57. Connelly, J.T., A.J. Garcia, and M.E. Levenston, *Inhibition of in vitro chondrogenesis in RGD-modified three-dimensional alginate gels.* Biomaterials, 2007. **28**(6): p. 1071-83.

58. Takahashi, I., et al., *Effect of stretching on gene expression of beta1 integrin and focal adhesion kinase and on chondrogenesis through cell-extracellular matrix interactions.* Eur J Cell Biol, 2003. **82**(4): p. 182-92.
59. Segat, D., et al., *Integrins alpha(6A)beta 1 and alpha(6B)beta 1 promote different stages of chondrogenic cell differentiation.* J Biol Chem, 2002. **277**(35): p. 31612-22.
60. Connelly, J.T., A.J. Garcia, and M.E. Levenston, *Interactions between integrin ligand density and cytoskeletal integrity regulate BMSC chondrogenesis.* J Cell Physiol, 2008. **217**(1): p. 145-54.
61. Lu, Z.F., et al., *Beta1 integrins regulate chondrogenesis and rock signaling in adipose stem cells.* Biochem Biophys Res Commun, 2008. **372**(4): p. 547-52.
62. Xia, M. and Y. Zhu, *Fibronectin fragment activation of ERK increasing integrin alpha(5) and beta(1) subunit expression to degenerate nucleus pulposus cells.* J Orthop Res, 2011. **29**(4): p. 556-61.
63. Homandberg, G.A., et al., *Antisense oligonucleotides to the integrin receptor subunit alpha(5) decrease fibronectin fragment mediated cartilage chondrolysis.* Osteoarthritis Cartilage, 2002. **10**(5): p. 381-93.
64. Loeser, R.F., et al., *Fibronectin fragment activation of proline-rich tyrosine kinase PYK2 mediates integrin signals regulating collagenase-3 expression by human chondrocytes through a protein kinase C-dependent pathway.* J Biol Chem, 2003. **278**(27): p. 24577-85.
65. Homandberg, G.A., V. Costa, and C. Wen, *Fibronectin fragments active in chondrocytic chondrolysis can be chemically cross-linked to the alpha5 integrin receptor subunit.* Osteoarthritis Cartilage, 2002. **10**(12): p. 938-49.
66. Gemba, T., et al., *Focal adhesion kinase and mitogen-activated protein kinases are involved in chondrocyte activation by the 29-kDa amino-terminal fibronectin fragment.* J Biol Chem, 2002. **277**(2): p. 907-11.
67. Ding, L., D. Guo, and G.A. Homandberg, *Fibronectin fragments mediate matrix metalloproteinase upregulation and cartilage damage through proline rich tyrosine kinase 2, c-src, NF-kappaB and protein kinase Cdelta.* Osteoarthritis Cartilage, 2009. **17**(10): p. 1385-92.
68. Su, S.L., et al., *Expression and regulation of Toll-like receptor 2 by IL-1beta and fibronectin fragments in human articular chondrocytes.* Osteoarthritis Cartilage, 2005. **13**(10): p. 879-86.
69. Li, X.Q., et al., *ITGBL1 Is a Runx2 Transcriptional Target and Promotes Breast Cancer Bone Metastasis by Activating the TGFbeta Signaling Pathway.* Cancer Res, 2015. **75**(16): p. 3302-13.
70. Gan, X., et al., *Epigenetic downregulated ITGBL1 promotes non-small cell lung cancer cell invasion through Wnt/PCP signaling.* Tumour Biol, 2016. **37**(2): p. 1663-9.
71. Sun, L., et al., *Extracellular matrix protein ITGBL1 promotes ovarian cancer cell migration and adhesion through Wnt/PCP signaling and FAK/SRC pathway.* Biomed Pharmacother, 2016. **81**: p. 145-151.
72. Wang, M., et al., *Characterization of gene expression profiles in HBV-related liver fibrosis patients and identification of ITGBL1 as a key regulator of fibrogenesis.* Sci Rep, 2017. **7**: p. 43446.
73. Yang, S., et al., *Hypoxia-inducible factor-2alpha is a catabolic regulator of osteoarthritic cartilage destruction.* Nat Med, 2010. **16**(6): p. 687-93.
74. Kim, J.H., et al., *Regulation of the catabolic cascade in osteoarthritis by the zinc-ZIP8-MTF1 axis.* Cell, 2014. **156**(4): p. 730-43.

75. Zhen, G., et al., *Inhibition of TGF-beta signaling in mesenchymal stem cells of subchondral bone attenuates osteoarthritis.* Nat Med, 2013. **19**(6): p. 704-12.
76. Candela, M.E., et al., *Alpha 5 Integrin Mediates Osteoarthritic Changes in Mouse Knee Joints.* PLoS One, 2016. **11**(6): p. e0156783.
77. Szabo-Rogers, H.L., et al., *New directions in craniofacial morphogenesis.* Dev Biol, 2010. **341**(1): p. 84-94.
78. Square, T., et al., *A gene expression map of the larval Xenopus laevis head reveals developmental changes underlying the evolution of new skeletal elements.* Dev Biol, 2015. **397**(2): p. 293-304.
79. Bonnard, C., et al., *Mutations in IRX5 impair craniofacial development and germ cell migration via SDF1.* Nat Genet, 2012. **44**(6): p. 709-13.
80. Minoux, M. and F.M. Rijli, *Molecular mechanisms of cranial neural crest cell migration and patterning in craniofacial development.* Development, 2010. **137**(16): p. 2605-21.
81. Pala, D., et al., *Focal adhesion kinase/Src suppresses early chondrogenesis: central role of CCN2.* J Biol Chem, 2008. **283**(14): p. 9239-47.
82. Rao, Z., et al., *Crystallization of a calcium-binding EGF-like domain.* Acta Crystallogr D Biol Crystallogr, 1995. **51**(Pt 3): p. 402-3.
83. Handford, P.A., et al., *The first EGF-like domain from human factor IX contains a high-affinity calcium binding site.* EMBO J, 1990. **9**(2): p. 475-80.
84. Malby, S., et al., *The first epidermal growth factor-like domain of the low-density lipoprotein receptor contains a noncanonical calcium binding site.* Biochemistry, 2001. **40**(8): p. 2555-63.
85. Fehon, R.G., et al., *Molecular interactions between the protein products of the neurogenic loci Notch and Delta, two EGF-homologous genes in Drosophila.* Cell, 1990. **61**(3): p. 523-34.
86. Cordle, J., et al., *Localization of the delta-like-1-binding site in human Notch-1 and its modulation by calcium affinity.* J Biol Chem, 2008. **283**(17): p. 11785-93.
87. Takagi, J., et al., *Global conformational rearrangements in integrin extracellular domains in outside-in and inside-out signaling.* Cell, 2002. **110**(5): p. 599-11.
88. Yan, B. and J.W. Smith, *A redox site involved in integrin activation.* J Biol Chem, 2000. **275**(51): p. 39964-72.
89. Ye, F., C. Kim, and M.H. Ginsberg, *Reconstruction of integrin activation.* Blood, 2012. **119**(1): p. 26-33.
90. Benya, P.D. and J.D. Shaffer, *Dedifferentiated chondrocytes reexpress the differentiated collagen phenotype when cultured in agarose gels.* Cell, 1982. **30**(1): p. 215-24.
91. McDougall, S., et al., *Surface adhesion-mediated regulation of chondrocyte-specific gene expression in the nontransformed RCJ 3.1C5.18 rat chondrocyte cell line.* J Bone Miner Res, 1996. **11**(8): p. 1130-8.
92. Norby, D.P., C.J. Malemud, and L. Sokoloff, *Differences in the collagen types synthesized by lapine articular chondrocytes in spinner and monolayer culture.* Arthritis Rheum, 1977. **20**(2): p. 709-16.
93. Tanaka, N., et al., *alpha5beta1 integrin induces the expression of noncartilaginous procollagen gene expression in articular chondrocytes cultured in monolayers.* Arthritis Res Ther, 2013. **15**(5): p. R127.
94. Tsolis, K.C., et al., *Comparative proteomic analysis of hypertrophic chondrocytes in osteoarthritis.* Clin Proteomics, 2015. **12**(1): p. 12.

95. Barilla, M.L. and S.E. Carsons, *Fibronectin fragments and their role in inflammatory arthritis.* Semin Arthritis Rheum, 2000. **29**(4): p. 252-65.
96. Murakami, S., V. Lefebvre, and B. de Crombrugghe, *Potent inhibition of the master chondrogenic factor Sox9 gene by interleukin-1 and tumor necrosis factor-alpha.* J Biol Chem, 2000. **275**(5): p. 3687-92.
97. Raymond, L., et al., *Interleukin-1 beta induction of matrix metalloproteinase-1 transcription in chondrocytes requires ERK-dependent activation of CCAAT enhancer-binding protein-beta.* J Cell Physiol, 2006. **207**(3): p. 683-8.
98. Jackson, M.T., et al., *Depletion of protease-activated receptor 2 but not protease-activated receptor 1 may confer protection against osteoarthritis in mice through extracartilaginous mechanisms.* Arthritis Rheumatol, 2014. **66**(12): p. 3337-48.
99. Kara, N., et al., *miR-27 regulates chondrogenesis by suppressing focal adhesion kinase during pharyngeal arch development.* Dev Biol, 2017. **429**(1): p. 321-334.
100. Onodera, K., et al., *Stepwise mechanical stretching inhibits chondrogenesis through cell-matrix adhesion mediated by integrins in embryonic rat limb-bud mesenchymal cells.* Eur J Cell Biol, 2005. **84**(1): p. 45-58.
101. Woods, A., G. Wang, and F. Beier, *Regulation of chondrocyte differentiation by the actin cytoskeleton and adhesive interactions.* J Cell Physiol, 2007. **213**(1): p. 1-8.
102. Henderson, B., et al., *Fibronectin: a multidomain host adhesin targeted by bacterial fibronectin-binding proteins.* FEMS Microbiol Rev, 2011. **35**(1): p. 147-200.
103. Ding, L., D. Guo, and G.A. Homandberg, *The cartilage chondrolytic mechanism of fibronectin fragments involves MAP kinases: comparison of three fragments and native fibronectin.* Osteoarthritis Cartilage, 2008. **16**(10): p. 1253-62.
104. Huang, H., et al., *Age-dependent Changes in the Articular Cartilage and Subchondral Bone of C57BL/6 Mice after Surgical Destabilization of Medial Meniscus.* Sci Rep, 2017. **7**: p. 42294.
105. Mathiessen, A. and P.G. Conaghan, *Synovitis in osteoarthritis: current understanding with therapeutic implications.* Arthritis Res Ther, 2017. **19**(1): p. 18.
106. Lowin, T. and R.H. Straub, *Integrins and their ligands in rheumatoid arthritis.* Arthritis Res Ther, 2011. **13**(5): p. 244.
107. Badger, A.M., et al., *Disease-modifying activity of SB 273005, an orally active, nonpeptide alphavbeta3 (vitronectin receptor) antagonist, in rat adjuvant-induced arthritis.* Arthritis Rheum, 2001. **44**(1): p. 128-37.
108. Yousry, T.A., et al., *Evaluation of patients treated with natalizumab for progressive multifocal leukoencephalopathy.* N Engl J Med, 2006. **354**(9): p. 924-33.
109. El Azreq, M.A., et al., *alpha2beta1 integrin regulates Th17 cell activity and its neutralization decreases the severity of collagen-induced arthritis.* J Immunol, 2013. **191**(12): p. 5941-50.